NeuroImage 119 (2015) 103–118

Contents lists available at ScienceDirect

NeuroImage

journal homepage: www.elsevier.com/locate/ynimg

Dynamic brain architectures in local brain activity and functional network efficiency associate with efficient reading in bilinguals

Gangyi Feng [a], Hsuan-Chih Chen [b], Zude Zhu [c], Yong He [d,e], Suiping Wang [a,f,*]

[a] Center for the Study of Applied Psychology and School of Psychology, South China Normal University, Guangzhou 510631, China
[b] Department of Psychology, Chinese University of Hong Kong, Hong Kong
[c] Collaborative Innovation Center for Language Competence, Jiangsu Normal University, Xuzhou 221009, China
[d] State Key Laboratory of Cognitive Neuroscience and Learning & IDG/McGovern Institute for Brain Research, Beijing Normal University, Beijing 100875, China
[e] Center for Collaboration and Innovation in Brain and Learning Sciences, Beijing Normal University, Beijing 100875, China
[f] Guangdong Provincial Key Laboratory of Mental Health and Cognitive Science, South China Normal University, Guangzhou 510631, China

ARTICLE INFO

Article history:
Received 30 September 2014
Accepted 27 May 2015
Available online 18 June 2015

Keywords:
Neuroimaging
Brain network
Graph theory
Reading
Bilingualism

ABSTRACT

The human brain is organized as a dynamic network, in which both regional brain activity and inter-regional connectivity support high-level cognitive processes, such as reading. However, it is still largely unknown how the functional brain network organizes to enable fast and effortless reading processing in the native language (L1) but not in a non-proficient second language (L2), and whether the mechanisms underlying local activity are associated with connectivity dynamics in large-scale brain networks. In the present study, we combined activation-based and multivariate graph-theory analysis with functional magnetic resonance imaging data to address these questions. Chinese–English unbalanced bilinguals read narratives for comprehension in Chinese (L1) and in English (L2). Compared with L2, reading in L1 evoked greater brain activation and recruited a more globally efficient but less clustered network organization. Regions with both increased network efficiency and enhanced brain activation in L1 reading were mostly located in the fronto-temporal reading-related network (RN), whereas regions with decreased global network efficiency, increased clustering, and more deactivation in L2 reading were identified in the default mode network (DMN). Moreover, functional network efficiency was closely associated with local brain activation, and such associations were also modulated by reading efficiency in the two languages. Our results demonstrate that an economical and integrative brain network topology is associated with efficient reading, and further reveal a dynamic association between network efficiency and local activation for both RN and DMN. These findings underscore the importance of considering interregional connectivity when interpreting local *BOLD* signal changes in bilingual reading.

Introduction

Reading is a high-level language process based on a set of co-activated cortical areas and dynamic inter-regional communication within a large-scale brain network. Such functional network organization and flexibility enable us to read in our native language (L1) effortlessly. Although the same neural underpinnings also support reading in a non-proficient second language (L2) (Abutalebi, 2008; Indefrey, 2006; Perani and Abutalebi, 2005), L2 reading is an exceptionally challenging task. It remains unclear how the human brain system supports such efficient reading in L1 but not in L2.

Using activation-based imaging approaches, previous studies have revealed a similar fronto-tempo-parietal network supporting reading comprehension across languages (Abutalebi, 2008; Chee et al., 1999b; Vigneau et al., 2006; Wartenburger et al., 2003), independent of surface differences between linguistic systems (Chee et al., 1999a; Nakamura et al., 2012). However, different activation patterns of these regions have been observed in L1 and L2 (Abutalebi, 2008; Perani and Abutalebi, 2005). Specifically, reduced regional activation in the frontal and parietal regions and greater activation in the temporal lobe regions have been observed in L1 as compared with L2 during reading comprehension (Chee et al., 2000; Perani et al., 1996; Ruschemeyer et al., 2005; Wartenburger et al., 2003; Yokoyama et al., 2006). As the fronto-parietal regions have been associated with cognitive control, the reduced local activation has been interpreted as reflecting reduced requirement for control processes during L1 reading. In contrast, greater activation in temporal regions suggests an association between regional activation and efficient or automatic L1 reading processing (Abutalebi, 2008; Indefrey, 2006).

The above cognitive mechanisms might provide an explanation for how local *BOLD* signal changes in these regions support efficient reading

* Corresponding author at: Center for the Study of Applied Psychology and School of Psychology, South China Normal University, Guangzhou 510631, China.
E-mail address: suiping@scnu.edu.cn (S. Wang).

http://dx.doi.org/10.1016/j.neuroimage.2015.05.100
1053-8119/

in L1. However, these regions do not activate independently in support of cognitive processes. Rather, the neural basis of efficient reading might be best characterized by the brain connectome instead of individual nodes' activities (Bullmore and Sporns, 2012; Friederici and Gierhan, 2013; Park and Friston, 2013). Specifically, reading comprises a series of cognitive components, from low-level orthographic/phonological processing to higher-level semantic processing, syntactic parsing, and situation model construction in discourse (Perfetti and Frishkoff, 2008). Implementing such complex cognitive processes requires efficient cooperation between reading-relevant regions and inhibition of other task-irrelevant systems for rapid and effective information communication (Friederici, 2012; Salmelin and Kujala, 2006). Using functional connectivity analysis, it has been found that reading ability in both children and adults is associated with the connection strength among reading-relevant regions (Koyama et al., 2011).

Two brain networks, the reading-related network (RN) (Koyama et al., 2010) and the default-mode network (DMN) (Greicius et al., 2003; Raichle et al., 2001), have been proposed to play important roles in reading comprehension. The RN consists of several regions consistently implicated during reading, including the inferior frontal gyrus, most of the temporal lobe regions, and part of the parietal lobe in both hemispheres (Price, 2010; Vigneau et al., 2006, 2011). But it must also be pointed out that, although for the sake of simplicity we used the term "reading-related network", there is evidence that not all regions in this network are necessarily functionally specified for reading alone (Price and Devlin, 2011; Vogel et al., 2012b; Ye and Zhou, 2009). For example, some regions that were consistently involved in a wide range of reading tasks fall under the fronto-parietal control network and the dorsal-attention network (Power et al., 2011; Price, 2010; Vigneau et al., 2006, 2011; Yeo et al., 2011); and they were intrinsically connected to each other, as revealed by the resting-state functional connectivity studies (Koyama et al., 2010; Tomasi and Volkow, 2012). In contrast, the DMN (Fox et al., 2005; Raichle et al., 2001) is consistently deactivated during reading and other cognitive tasks, and is comprised of the posterior cingulate cortex, medial prefrontal cortex, inferior parietal lobe, and lateral temporal cortex, suggesting an association with internal mental processing (Anticevic et al., 2012; Raichle, 2010) and semantic cognition (Binder et al., 2009). Resting-state functional MRI signals from the two networks are anti-correlated (Koyama et al., 2010), suggesting functional interactions between them. However, it is still unclear how the interaction and association between these networks support efficient reading.

Using a powerful approach known as graph-theory analysis (GTA) (Bullmore and Sporns, 2009; He and Evans, 2010), both connectivity profiles and network efficiency can be quantified by examining how efficiently individual nodes integrate signals at local and global levels. Previous studies using GTA have consistently shown that the brain network is optimally organized in a 'small-world' topology with dense intra-modular connections and relatively few inter-modular connections (Bullmore and Bassett, 2011; Bullmore and Sporns, 2009; He and Evans, 2010). Researchers have further found that the efficiency of network organization is associated with task performance in both language (Sheppard et al., 2012) and general cognitive tasks (Giessing et al., 2013; Kitzbichler et al., 2011). Moreover, regions co-activated or co-deactivated during a cognitive task are consistently organized as a functional network community with dense inter-regional connections and are associated with similar cognitive functions (Crossley et al., 2013; Laird et al., 2011). For instance, it has been observed that regions activated during a Go/Nogo task partially overlap with regions showing increased network efficiency in the resting-state that follows the task. Furthermore, this increased efficiency is associated with better task performance (Giessing et al., 2013, but see Tomasi et al., 2014).

The evidence mentioned above suggests that efficient cognitive processing may be associated with both optimal brain network organization and the dynamics between functional connectivity and local brain activation. Yet, there is a lack of direct evidence as to whether this optimized network and its dynamics support efficient reading processing. To this end, in the present study we collected functional MRI data from 40 Chinese–English unbalanced bilinguals reading narratives for comprehension in both Chinese (L1) and English (L2). With such a design, we were able to investigate not only how the functional network topology supports efficient reading by contrasting L1 with L2, but also how the network topology supports L2 reading by taking individual differences into account. Specifically, by combining GTA and univariate activation-based analysis (focusing on the networks activated (RN) and deactivated (DMN) during reading), we first quantitatively compared brain network efficiency as well as local activation between languages. We hypothesized that not only is the activation of reading-relevant regions during reading tasks important for reading, but also the optimization of connectivity patterns across regions is crucial for efficient reading processing. We then examined the association between network efficiency and local brain activation, and further investigated whether such association might be modulated by how efficiently the language is processed. These analyses may help further our understanding of brain dynamics, at both local and network scales, and of how these dynamics underlie efficient reading.

Materials and methods

Participants

Forty healthy Chinese–English bilinguals participated in the fMRI experiment (10 males; age = 23.2 ± 1.5 [mean ± SD] years). They were all right-handed, with normal or corrected-to-normal vision, and without neurological impairment, as confirmed by questionnaires and short interviews. All participants were native speakers of Chinese who started to learn English as their second language after 10 years of age (mean age of acquisition, AOA = 12.2 years old). With the exception of two participants, all of them had previously passed the CET-4 (level 4 of College English Test). This indicates that all participants had a low-to-intermediate level of English proficiency.

Participants were asked to report their language proficiency on a 7-point scale (1 for "*very non-proficient*", 7 for "*very proficient*") for both of their languages. On average, the participants rated themselves as non-proficient to moderately-proficient unbalanced bilinguals (mean score: English = 3.45 [SD = 1.32], Chinese = 6.23 [SD = 0.93], $P < .01$), which was in accordance with their CET-4 scores. We subsequently asked them to finish a questionnaire, estimating their exposure time to each language in different situations, including media (television, radio and internet), family (with all members), university (in class and at work), friends (outside of class), reading (newspapers and books), and other activities (music, hobbies, sports, etc.), which covered listening, speaking, reading and writing in their daily life (Wartenburger et al., 2003). The results confirmed that all participants spent significantly more time using Chinese than they did using English in all categories ($Ps < .01$). Before the experiment, all participants signed written consent forms approved by the institutional review boards of South China Normal University and Southwest University.

Stimuli and procedure

Two English stories chosen from A Collection of English Readings (Jia, 2002) were used as stimuli in the fMRI experiment ("Farmer Lum", page 56; "Twelfth Night (I)", page 156). Another story from the same book was used as practice material before the fMRI experiment ("A Kind-hearted Drunk", page 124). Original stories in English were modified by two high-proficiency English major students, replacing low-frequency words and uncommon syntactic structures, to ensure that all participants could understand the content of the stories. These stories were then translated into Chinese to serve as the Chinese-language stimuli (see Table 1 for samples). In the final version of the experimental materials, each story had two versions, one in English and

Table 1
Narrative stimuli samples in both language conditions.

Condition	Samples
Chinese (L1)	… 船长告诉薇拉他看见塞伯辛在船沉没前将自己绑在一块结实的木头上了。所以他也是有希望获救的。这是个好消息,薇拉渐渐地感觉好些了。…
English (L2)	… The captain told her that he had seen Sebastian tie himself to a strong piece of wood before the ship sank. There was a chance that he had been saved also. This was good news, and Viola began to feel happier. …

one in Chinese. The English version of Story 1 contained 742 words, while the Chinese version contained 1351 Chinese characters that can be divided into 716 meaningful constituents. The English version of Story 2 had 730 words, while its Chinese version had 1365 Chinese characters or 710 constituents.

A blocked design was employed in the fMRI experiment (see Fig. 1A). We presented one story in each run, which lasted a total of 12.2 min, including a 30-s resting period before and after each story presentation. Each run was composed of 13 reading blocks (35.5 s on average for each block) and 12 resting blocks that were inserted between every two reading blocks. To limit the potential confounds induced by alternating between reading and resting blocks, we divided each story into blocks according to its plot, making sure that each reading block covered a paragraph or a locally-coherent part of the story. Because the number of words/constituents was not identical between the English and Chinese versions of the same story, the total duration of reading blocks varies slightly. Therefore, we adjusted the duration of each resting block to make sure that both the total scanning time and the reading speed of each story were identical in the two different languages. Thus, the duration of each resting block is dependent on the duration of the preceding reading block (mean duration of resting block: 17.5 s, range from 14 to 22 s).

E-Prime software package (Psychology Software Tools, Pittsburgh, PA; version 2.0) was used for stimulus presentation and behavioral data collection. Using the rapid serial visual presentation procedure (RSVP), narrative stimuli were presented word-by-word or constituent-by-constituent onto a screen within the MRI-cabin by a MRI-compatible LCD projector. Each word/constituent lasted 300 ms and the punctuation marks were presented together with the closest word/constituent. Different inter-stimulus intervals were used between different constituents, depending on the position of the constituents in a sentence: the duration was 100 ms for constituents in the middle of a sentence, 500 ms for constituents ending with a comma, and 1500 ms for constituents ending with a period. This presentation procedure was determined by a pilot experiment that used a self-paced reading paradigm to define a more natural speed of RSVP procedure. To minimize the confounding of cross-language interference caused by the previous story (Elston-Güttler et al., 2005), the languages were presented in different orders counterbalanced across participants.

Participants were instructed that they would participate in a narrative reading comprehension experiment. They were asked to lie in a supine position inside the MRI scanner while wearing MRI-compatible earphones and holding a button box. They were told not to move their head (which was restrained by padding) while inside the MRI scanner. During the fMRI experiment, they read two different narratives in the two languages, one in Chinese and the other in English, and then judged the validity of 10 statements about the stories' contents one by one at the end of each story. Each statement was presented on the center of the screen, and participants needed to press a button to judge whether the statement was correct or incorrect within 5 s. To make sure that the participants understood the instructions correctly and were familiar with the procedure, we asked them to read a practice story outside the scanner before undergoing fMRI scanning.

MRI data acquisition

Imaging data were acquired using a Siemens Trio 3T MRI system with a standard head coil located at the Cognition and Personality Key Laboratory of the Ministry of Education at Southwest University in China. Three functional runs, generating 366 images each, were performed first, followed by a structural imaging run. A resting-state fMRI run was also acquired prior to the two narrative reading runs. During the functional runs, the whole-brain blood oxygen level-dependent (*BOLD*) signals were recorded by a T2*-weighted gradient echo-planar imaging (EPI) pulse sequence using an interleaved scanning method (TR = 2000 ms, TE = 30 ms, flip angle = 90°, 32 slices, slice thickness = 4 mm, voxel size $3 \times 3 \times 4$ mm^3). In the structural imaging

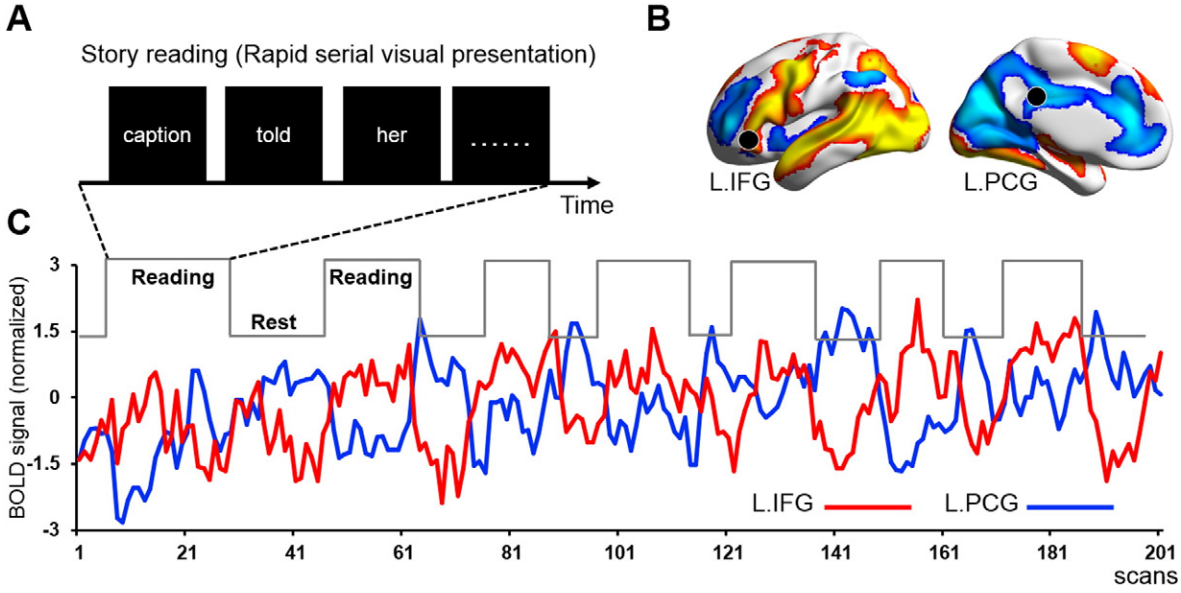

Fig. 1. Experimental design and brain activity evoked by reading. A, story reading paradigm. Each word of the narratives was presented onto the screen one by one during the Reading blocks. B, Brain activation (yellow-red) and deactivation (light blue-dark blue) during reading. C, Fraction of time-course in two representative regions (LIFG and LPCG) were showed continually task-related activity and task-unrelated activity, respectively. LIFG, left inferior frontal gyrus; LPCG, left posterior cingulate gyrus.

run, T1-weighted high resolution structural images were acquired for each subject using an MP-RAGE sequence (192 slices, TE = 3.03 ms; slice thickness = 1 mm; voxel size $1 \times 1 \times 1$ mm^3).

Univariate activation analysis

All imaging data were preprocessed using SPM8 (Wellcome Department of Imaging Neuroscience, London, UK; www.fil.ion.ucl.ac.uk/spm/). The initial five images of the functional data were discarded to improve the equilibrium state of magnetization. Next, brain scans were corrected for head movement by spatially realigning them with the first brain volume, and mean functional images were computed. In all scans, head movement was within the acceptable range of 2 mm translation and 2 degree rotation in any direction. No participant's data were thus removed from the subsequent analysis. To normalize functional images, the mean functional image was coregistered with the structural image and segmented for each participant. The parameters obtained in the segmentation step were used to normalize the functional images onto the Montreal Neurological Institute space. Finally, normalized images were resampled into a spatial resolution of $2 \times 2 \times 2$ mm^3 and smoothed with a Gaussian kernel of 6-mm full width at half maximum.

Whole-brain statistical analysis was performed using general linear modeling (GLM) for the subject-level and random effect models for the group-level. To locate the brain regions modulated by story reading in the two languages, four regressors were included in the SPM design matrix: English story reading blocks (EN_S), English resting blocks (EN_R), Chinese story reading blocks (CH_S), and Chinese resting blocks (CH_R). The onsets and durations of each type of block were convolved with the canonical hemodynamic response function (HRF) to build a general linear model. Six head movement parameters were included as nuisance regressors to minimize the motion related artifacts. Four contrasts of interest, (CH_S–CH_R), (EN_S–EN_R), ([CH_S–CH_R]–[EN_S–EN_R]), and ([EN_S–EN_R]–[CH_S–CH_R]) were calculated for each participant and subsequently entered into group-level analyses. Furthermore, we performed conjunction analyses for identifying the common regions that were activated ([CH_S–CH_R] & [EN_S–EN_R]) and deactivated ([CH_R–CH_S] & [EN_R–EN_S]) in both language. A false discovery rate (FDR) corrected threshold of $P = .05$ was used for all contrasts.

Data preprocessing for graph-theory analysis

In GTA, the preprocessing procedures were applied in the same manner as they were for the univariate activation analysis. In order to exclude effects due to stimulus presentation, we only analyzed the residuals ε of the general linear model of $KY = KX\beta + \varepsilon$ where Y denotes the fMRI time-series in each voxel, X represents the matrix of word presentation onsets that is convolved with the hemodynamic function, K is a Gaussian smoothing matrix, and ε is the residual error. This method has been used in other functional connectivity studies for excluding stimulus-related fluctuations (Fair et al., 2007; Lohmann et al., 2010). Then we applied temporal band-pass filtering ($0.008 < f < 0.1$ Hz) to the residuals to reduce low-frequency drift and high-frequency physiological noises (Cordes et al., 2001). Finally, nuisance signals, including averaged whole-brain signals, cerebral white matter, and cerebrospinal fluid, as well as six direction head movement parameters, were linearly regressed out of the functional time series.

Brain network construction and threshold selection

Using graph theory, the human brain network is abstracted and modeled as a graph, which is composed of a set of nodes linked by edges. In the graph-theory analysis of fMRI data, nodes represent a set of regions or voxels, and edges represent the functional connectivity between those nodes (Bullmore and Bassett, 2011; Bullmore and Sporns, 2009). In this study, to define the nodes of the brain network, we divided the preprocessed images into a set of regions using two gray-matter templates. Given that different parcellation templates and nodal scales may result in considerable variation of network metrics (Fornito et al., 2010; Wang et al., 2009), we used two templates to cross-validate our results. Both templates are defined by the atlas of Automated Anatomical Labeling (Tzourio-Mazoyer et al., 2002), but in different nodal resolutions. One template, AAL-90, is composed of 90 regions (45 regions in each hemisphere, see Table 2 for details), and the other, AAL-1024, is composed of 1024 regions (512 regions in each hemisphere). Subsequently, representative mean time series for each node were extracted from the preprocessed data for each run by averaging all voxel time series within that region. Next, to define network edges, functional connectivity between all possible pairs of nodes was measured by calculating Pearson's correlation coefficients. As a result, a 90×90 correlation matrix (AAL-90 template) and a 1024×1024 correlation matrix (AAL-1024 template) were obtained for each participant. Finally, a specified threshold was applied to each correlation matrix to convert it into an unweighted binary adjacency matrix: if the absolute value of the correlation between any pair of nodes was greater than the given threshold, then an edge (represented by a 1 in the adjacency matrix) was constructed between that pair, otherwise no edge was constructed (represented by a 0). We used the sparsity threshold approach, a wide range of network densities, to threshold all of the correlation matrices and generate the binary matrices. Connection sparsity (i.e., connection cost) is defined as the ratio of the number of existing edges divided by the number of all possible edges in the graph. For example, if we set cost = 0.1, the strongest 10% of connections would be preserved. This unbiased approach enabled us to directly compare network metrics between conditions while minimizing possible confounds that would result from the use of a single fixed threshold (Bullmore and Bassett, 2011). As previous findings have shown that networks with high connection cost (>0.5) tend to be less meaningful biologically, and low connection cost tend to result in a fragmented network organization (Achard and Bullmore, 2007; Bullmore and Bassett, 2011; Bullmore and Sporns, 2012), we selected costs within the range of 0.06–0.5, increasing with a regular increment of 0.02, to threshold each correlation matrix. All network metrics were calculated separately for each binary network in this pre-defined cost range.

Network metrics

Three network metrics, global efficiency (E_{glob}), local efficiency (E_{loc}), and maximal cost-efficiency (CE_{max}), were the main focus of the graph-theory analysis. The conventional "small-world" organization measures (Watts and Strogatz, 1998), including characteristic path length (L_p), normalized L_p (λ), clustering coefficient (C_p), normalized C_p (γ) and small-worldness index Sigma ($\sigma = \gamma/\lambda$) were also calculated as references for determining if the network fell within the "small-world" regime ($\sigma > 1$) (Bullmore and Bassett, 2011).

Global efficiency is a network topological metric that can measure the efficiency of parallel information transfer within a given graph G. $E_{glob}(i)$ represents the global efficiency of an individual node i and is defined as follows:

$$E_{glob}(i) = \frac{1}{N-1} \sum_{i \neq j \in G} \frac{1}{L_{ij}}$$

where N denotes the total number of nodes within G, and L_{ij} denotes the shortest path length between nodes i and j. Thus, $E_{glob}(i)$ is the average of the inverse shortest path lengths from node i to all other nodes. This measure is superior to the conventional characteristic path length L_p (averaged L_{ij} across all network nodes, Watts and Strogatz, 1998) because it allows the computation of a finite value for graphs with disconnected nodes, as well as accounting for how efficiently the network transfers information in parallel between network nodes (Latora

Table 2
Brain regions that used as nodes for constructing functional network graphs in the AAL-90 template.

Regions	Abbreviation	Regions	Abbreviation
Precentral gyrus	PreCG	Lingual gyrus	LING
Superior frontal gyrus (dorsal)	SFGdor	Superior Occipital gyrus	SOG
Orbitofrontal cortex (superior)	ORBsup	Middle occipital gyrus	MOG
Middle frontal gyrus	MFG	Inferior occipital gyrus	IOG
Orbitofrontal cortex (middle)	ORBmid	Fusiform gyrus	FFG
Inferior frontal gyrus (opercular)	IFGoperc	Postcentral gyrus	PoCG
Inferior frontal gyrus (triangular)	IFGtriang	Superior parietal gyrus	SPG
Orbitofrontal cortex (inferior)	ORBinf	Inferior parietal lobule	IPL
Rolandic operculum	ROL	Supramarginal gyrus	SMG
Supplementary motor area	SMA	Angular gyrus	ANG
Olfactory	OLF	Precuneus	PCUN
Superior frontal gyrus (medial)	SFGmed	Paracentral lobule	PCL
Orbitofrontal cortex (medial)	ORBmed	Caudate	CAU
Rectus gyrus	REC	Putamen	PUT
Insula	INS	Pallidum	PAL
Anterior cingulate gyrus	ACG	Thalamus	THA
Dorsal cingulate gyrus	DCG	Heschl gyrus	HES
Posterior cingulate gyrus	PCG	Superior temporal gyrus	STG
Hippocampus	HIP	Temporal pole (superior)	TPOsup
Parahippocampal gyrus	PHG	Middle temporal gyrus	MTG
Amygdala	AMYG	Temporal pole (middle)	TPOmid
Calcarine cortex	CAL	Inferior temporal gyrus	ITG
Cuneus	CUN		

Forty-five cortical and subcortical regions in each hemisphere were represented as network nodes, as defined by the atlas of Automated Anatomical Labeling.

and Marchiori, 2001). Larger E_{glob} indicates higher efficiency of signal communication, i.e., fewer processing steps between global brain network nodes.

The local efficiency measures the communication efficiency of a sub-graph with locally connected nodes. $E_{loc}(i)$ is the global efficiency calculated for G_i, the sub-graph composed of the directly connected neighbors of node i, and is defined as follows:

$$E_{loc}(i) = \frac{1}{N_{G_i}(N_{G_i}-1)} \sum_{j,k \in G_i} \frac{1}{L_{jk}}$$

where N_{Gi} is the number of nodes within the G_i, excluding node i itself (Achard and Bullmore, 2007; Latora and Marchiori, 2001). This metric is similar to the conventional clustering coefficient that measures how clustered the nodes of the network are, but E_{loc} also shows how efficient local communication is between the neighbors of node i (Achard and Bullmore, 2007).

We also investigated the economical properties of the generated networks by calculating maximal cost-efficiency (CE_{max}), where cost-efficiency (CE) is defined as follows:

$$CE = E_{glob} - cost$$

In the pre-defined range of connection costs, there will typically be a maximal value of CE, which is denoted as CE_{max}. CE_{max} is a metric independent of any specific threshold choice and has been observed to be a useful measure of network economy (Achard and Bullmore, 2007; Sheppard et al., 2012). All the above-mentioned nodal metrics were calculated at a whole-brain level by averaging them across all network nodes.

Finally, we used modular partition analysis to identify the RN and DMN based on the connectivity pattern, and further investigated whether L1 and L2 reading exhibit similar or different functional network community topologies (Bullmore and Sporns, 2009; He et al., 2009). A module is defined theoretically as a set of densely interconnected nodes with sparse connections to nodes in other modules (Fortunato, 2010). Previous studies have estimated this modular organization by calculating a quantitative parameter known as modularity, Q (Newman, 2006). Here, we used the heuristic modularity maximizing algorithm known as the Louvain algorithm, proposed by Blondel et al. (2008), to calculate the optimized Q and partition network nodes into sets of modules.

Statistical comparison of network properties between languages

For statistical analyses of those network metrics, we chose a range of connection costs according to two criteria: (1) at least 95% of the nodes were connected; (2) all constructed networks needed to be within the "small-world" regime ($\sigma > 1$) for each participant. These criteria ensured the resulting brain graphs had maximally connected nodes while simultaneously exhibiting "small-world" properties. As a result, we selected the cost range from 0.1 to 0.5 in both template schemas. In addition, we calculated the areas under the curve (AUC) of all network metrics over the selected cost range. This procedure provides a summarized measure for each network metric independent of any specific threshold choice (Achard and Bullmore, 2007), and has been demonstrated to be sensitive to differences between networks (Wang et al., 2009; Zhang et al., 2011).

To determine whether narrative reading in L1 exhibits different network properties from that of L2, both at whole-brain and nodal levels, we first compared the AUC of E_{glob}, E_{loc}, L_p, C_p, and modularity Q of L1 and L2, as well as CE_{max} at the whole-brain level by using nonparametric permutation tests (Nichols and Holmes, 2002). Specifically, we calculated the mean difference between the two language conditions for each network metric. To test the null hypothesis that the observed language differences occurred by chance, we randomly assigned all the values into two new conditions and recalculated the mean differences between the two randomized conditions. This randomization procedure was repeated 50,000 times, and the 95th percentile points of each distribution were used as the critical values for a two-tailed t test of the null hypothesis with $P = .05$. Before the permutation tests, multiple linear regression analyses were applied to remove the confounding effects of age, gender, age of acquisition of L2, L2 proficiency (normalized CET-4 scores), and story reading comprehension performance in both languages, for each network metric. Afterwards, to search for nodes that contributed to the observed differences in whole-brain network metrics, we compared L1 to L2 in nodal E_{glob} and E_{loc} using the procedure described above. Similar data analysis procedures have been used in other graph-theoretical studies (Fornito et al., 2011; Uehara et al., 2014).

Group-level partition and regions of interest analysis

In this study, we observed reading-related network (RN) and default-mode network (DMN) were activated and deactivated during narrative reading, respectively (see Fig. 2). To identify the RN and DMN modules based on the functional connectivity patterns for further regions of interest (ROI) analysis, we applied a group-level network partition analysis. A group-level correlation matrix was obtained by averaging Fisher's *r*-to-*z* transformed correlation matrices across languages and participants (He et al., 2009). Then, we constructed a group-level binary graph using a connection cost threshold of 0.247 for AAL-90 and of 0.153 for AAL-1024. We chose these two connection costs because participants' functional brain networks reached their maximal cost-efficiency at these two values. That is, the function networks were close to the optimal cost-efficiency organization at these costs. Afterwards, the graphs were partitioned into modules by applying the Louvain algorithm, as mentioned above (Blondel et al., 2008).

To further investigate the differences in network topology and local brain activity between L1 and L2 reading, we performed ROI analyses on RN and DMN ROIs that were identified by the previously-mentioned modular partition analysis. RN ROI was constructed by combining all the regions within RN module into one large ROI. Similarly, the DMN ROI was constructed by combining all regions within DMN module. Then, we extracted and averaged the E_{glob}, E_{loc}, and activation amplitude (Reading condition minus Rest condition) for each ROI, and further performed nonparametric permutation tests to compare these measures between L1 and L2 at group level. Note that while the modular partition was similar for both templates, all ROIs chosen here were based on the AAL-90 template.

Correlation between network efficiency and local BOLD signal changes

We further employed cross-region and cross-subject correlation analyses to directly investigate the relationship between local *BOLD* signal changes and network topological efficiency. Firstly, the mean effect size of reading-related activity (Reading minus Rest) was extracted for each voxel. We then averaged the values of all voxels within each parcellated region on the AAL-90 template. Secondly, the values of E_{glob}, E_{loc} and local *BOLD* signal changes were transformed into *z*-scores. Finally, both cross-region and cross-subject partial correlation analyses were used to calculate the correlation value between local *BOLD* signal changes and E_{glob} (*BOLD*-E_{glob} correlation), and between local *BOLD* signal changes and E_{loc} (*BOLD*-E_{loc} correlation). In the cross-region correlation analysis, we separated 90 regions (only the AAL-90 template was used) into two groups based on their activation pattern. One group of regions was activated, the other was deactivated during reading. Correlation analyses were applied separately for the two groups of regions. In the cross-subject correlation analysis, we only focused on two network modules, RN and DMN. At the network level, to probe the functional interaction between networks, we conducted correlation analyses on both local *BOLD* signal changes and network efficiency measures, and further associated them with reading performance. At the nodal level, we did similar analyses to further localize specific regions exhibiting significant *BOLD*-E_{glob} and *BOLD*-E_{loc} correlations, in which we controlled for potential confounding variables, including age, gender and age of acquisition of L2. A FDR procedure (Genovese et al., 2002) was used for multiple testing correction in all statistical comparisons (FDR corrected $P = .05$).

Finally, we investigated whether the *BOLD*-E_{glob} and *BOLD*-E_{loc} correlations within the RN and DMN modules were modulated by language (i.e., *BOLD*-E_{glob} or *BOLD*-E_{loc} correlations differed between languages). If this is the case, both RN and DMN might be separated into two subsystems, one system showing common *BOLD*-E_{glob} or *BOLD*-E_{loc} correlation across languages, the other showing language modulation effect. Therefore, we compared the Fisher *z*-transformed *BOLD*-E_{glob} and *BOLD*-E_{loc} correlations between the two languages using the following formula:

$$Z = \frac{z_1 - z_2}{\sqrt{\frac{1}{n_1 - 3} + \frac{1}{n_2 - 3}}}$$

In this equation, z_1, n_1 and z_2, n_2 denote the Fisher *z*-score-transformed correlation coefficients and number of subjects for L1 and L2, respectively. The null hypothesis is that no difference exists between the two language for the magnitude of the *BOLD*-E_{glob} or *BOLD*-E_{loc} correlations. *Z*-statistics were then transformed into *P*-values and the significance level was set at $P < .05$.

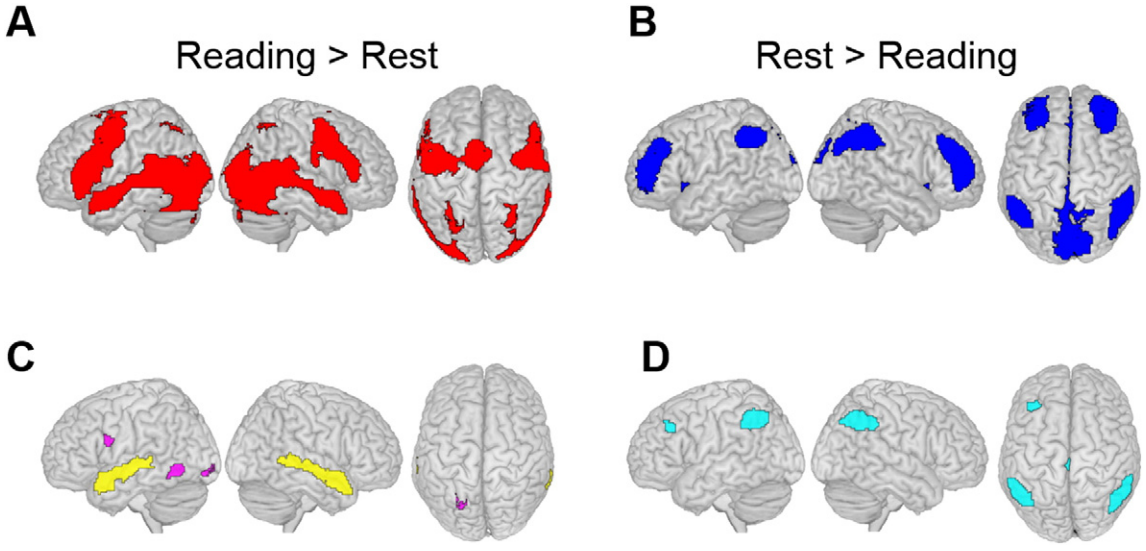

Fig. 2. Common and modulation effects of local brain activation between languages. A, brain regions that showed significant activation (left, Reading > Rest), and B, deactivation (right, Rest > Reading) during reading in both languages (conjunction analysis, see details in Materials and methods section). C, regions that showed significantly differences on local activities between L1 and L2 within the activated regions. Yellow regions represent L1 > L2; Pink regions represent L2 > L1. D, regions that showed significantly differences on local activities between L1 and L2 within the deactivated regions. Cyan regions represent more deactivation in L2 as compared with L1. Detailed brain regions were listed in Table 3. Voxel-level $P < .001$ and cluster-level FDR corrected at $P < .05$ were used in all contrasts. Left rendered brain is left hemisphere; Right rendered brain is right hemisphere.

Table 3
Brain regions that showed language modulation effect on regional brain response during story reading.

Activation patterns	Region	BA	MNI			peak *T*	voxels
			x	y	z		
Activation	**L1 > L2**						
	L. MTG/STG	21/22/38	−58	−8	−4	7.14	976
	L. FFG	37	−38	−50	−18	6.13	151
	R. MTG/STG	21/22/38	58	0	−8	6.39	1126
	L2 > L1						
	L. PreCG/IFG	6/9	−38	6	24	4.42	151
	L. Precuneus/SPL	7	−22	−62	46	5.51	385
	L. ITG	37	−48	−58	−6	5.76	214
	L. LG	18	−16	−92	−8	8.10	273
Deactivation	**L1 > L2**						
	L. MFG	9	−34	28	40	5.19	103
	L. SMG/IPL	40/39	−58	−54	42	7.47	563
	L. MCG	31	−2	−26	44	4.20	104
	R. SMG/IPL	40/39	48	−64	44	6.33	568
	L2 > L1						
	None						

Activation, regions that showed enhanced *BOLD* signal changes during reading. *Deactivation*, regions that showed enhanced *BOLD* signal changes during resting. Significance voxel-level of $P < .001$ (uncorrected), cluster-level FDR corrected threshold at $P < .05$. Abbreviation: L., left hemisphere; R., right hemisphere. IFG, inferior frontal gyrus; MFG, middle frontal gyrus; PreCG, precentral gyrus; MTG, middle temporal gyrus; STG, superior temporal gyrus; SMG, supramarginal gyrus; IPL, inferior parietal lobule; SPL, superior parietal lobule; ITG, inferior temporal gyrus; FFG, fusiform gyrus; LG, lingual gyrus; MCG, middle cingulate gyrus.

Results

Reading comprehension performance

The accuracy in the narrative reading comprehension task were 90% ($SD = 7$) for L1 (Chinese) and 79% ($SD = 18$) for L2 (English). Reading performance in both language was significantly higher than chance (50%, $Ps < .01$), which indicates that participants did focus on the reading and understood most of the content of the narratives. Reading performance in Chinese was significantly better than that in English, $t(1,39) = 3.87$, $P < .01$, suggesting that narrative comprehension in L1 is better than that in L2 for participants with low-to-intermediate L2 proficiency.

fMRI activation results

Fig. 2 shows the activated (Fig. 2A) and deactivated (Fig. 2B) regions that are shared by both languages during reading. As compared with the Rest condition, narrative reading activated similar regions spanning frontal, temporal, parietal and visual cortices in both languages. In contrast, common deactivation spanned the bilateral prefrontal gyrus, medial frontal gyrus, bilateral inferior parietal gyrus, and precuneus. Of greater interest were the regions modulated by reading in the different languages. We focused on the differences between languages in the above-mentioned activated and deactivated regions, and further divided the language-modulated regions into two groups based on their activation and deactivation patterns. Within the reading-evoked activated regions, reading in L1 showed enhanced activation mainly located in the bilateral superior/middle temporal gyrus and left fusiform gyrus as compared with reading in L2 (Fig. 2C, yellow regions). In the reverse contrast (L2 > L1), enhanced activation was observed in the inferior frontal and occipito-temporal cortices during L2 reading (Fig. 2C, pink regions). On the other hand, of the regions deactivated during reading, those that showed more deactivation in L2 were prominent in the left dorsal prefrontal gyrus, bilateral inferior parietal gyrus, and middle cingulate gyrus (Fig. 2D, see Table 3 for detailed regions). However, no regions showed more deactivation during L1 reading. To further verify whether the difference between L1 and L2 on reading performance could have potentially confounded these activation findings, we performed a group-level analysis in which we included both accuracy and age as covariates. The results showed that including the two variables as covariates did not significantly change the original findings.

Differences in whole-brain functional network characteristics between languages

Table 4 summarizes the statistical results of E_{glob}, E_{loc}, L_p, C_p, modularity Q, and CE_{max} in the two languages. After the confounding variables (age, sex, AOA, reading performance) were regressed out, we still observed significant language modulation effects on five of the examined network metrics. Specifically, the network observed during L1 reading exhibited significantly increased E_{glob}, CE_{max}, and decreased L_p as compared with that observed during L2 reading under both templates. In contrast, moderately increased E_{loc} (only reached significance in AAL-1024 template) and significantly increased C_p were observed during L2 reading. The modular organization (modularity Q) did not show a significant change between languages, but a trend of increasing modularity for L2 reading was observed. To further verify whether the regression of stimulus onset variances could have biased the results in any substantial way, we reanalyzed these network measures on the original preprocessed data without the regression procedure. The language differences (L1 vs. L2) in all the network measures under the raw data analysis remain the same as the analysis using the residual time series (see Table S1 in Supplemental Materials). These converging results

Table 4
Language differences of six whole-brain network metrics in the two templates.

AAL-90					AAL-1024			
Metrics	L1	L2	*t*-value	*P*	L1	L2	*t*-value	*P*
E_{glob}	0.243 (0.006)	0.239 (0.009)	4.00	0.0002	0.251 (0.005)	0.249 (0.005)	3.46	0.0007
E_{loc}	0.296 (0.007)	0.298 (0.006)	1.36	0.1814	0.301 (0.007)	0.303 (0.008)	2.50	0.0170
CE_{max}	0.346 (0.017)	0.335 (0.021)	4.49	0.0001	0.388 (0.016)	0.382 (0.018)	3.06	0.0041
L_p	0.685 (0.031)	0.705 (0.045)	3.83	0.0003	0.693 (0.010)	0.698 (0.013)	2.34	0.0243
C_p	0.222 (0.014)	0.230 (0.014)	4.05	0.0002	0.210 (0.014)	0.217 (0.016)	2.87	0.0070
Modularity Q	0.184 (0.011)	0.187 (0.010)	1.39	0.1668	0.173 (0.010)	0.176 (0.010)	1.92	0.0613

For E_{glob}, E_{loc}, L_p, C_p and modularity Q, the values represent the mean areas under the curve (AUC) of these metrics over the connection cost range from 0.1 to 0.5. Numbers enclosed in parentheses are standard deviation of the mean.

suggest that the network involved in reading narratives in L1 exhibits a more globally efficient organization with lower connection cost than that involved in L2 reading, whereas the network involved in L2 reading exhibits a more clustered network topology.

Differences in nodal network efficiency between languages

To search for nodes showing significant differences in network efficiency between languages, we performed comparisons between L1 and L2 reading on the nodal E_{glob} as well as the nodal E_{loc}. Fig. 3 displays regions that showed significant language differences on E_{glob} and E_{loc} using both the AAL-90 and the AAL-1024 templates.

During L1 reading, several regions showed significantly increased E_{glob}, including the left superior temporal gyrus, bilateral middle temporal pole, bilateral hippocampus, and right middle temporal gyrus using the AAL-90 template (see Table 5 for detailed regions on AAL-90 template). Similar regions with increased E_{glob}, especially bilateral anterior superior temporal gyrus, were observed when using the AAL-1024 template. Moreover, benefiting from the higher spatial resolution of the AAL-1024 template (Hayasaka and Laurienti, 2010), we also found several regions showing significantly increased E_{glob} in L2 reading, including the left posterior inferior frontal gyrus and the left posterior inferior temporal gyrus. For nodal E_{loc}, no regions showed a significantly increased value during L1 reading in either of the templates. However, increased E_{loc} in the L2 reading was observed in the left middle orbitofrontal cortex, bilateral anterior cingulate gyrus, right medial orbitofrontal cortex, bilateral anterior inferior temporal gyrus, and bilateral inferior parietal gyrus across templates.

Table 5
Regions that showed significant language differences in regional AUC of E_{glob} and E_{loc} in the AAL-90 template.

E_{glob}				E_{loc}			
Regions	*t*-value	*P*	Direction	Regions	*t*-value	*P*	Direction
L. STG	4.31	0.0079	L1 > L2	L. ORBmid	3.93	0.0182	L2 > L1
L. TPOmid	4.33	0.0074	L1 > L2	L. ACG	3.63	0.0491	L2 > L1
L. HIP	4.50	0.0042	L1 > L2	R. ACG	4.88	0.0007	L2 > L1
R. MTG	4.47	0.0048	L1 > L2	R. REC	3.69	0.0414	L2 > L1
R. TPOmid	4.33	0.0074	L1 > L2				
R. HIP	5.09	0.0008	L1 > L2				

Regions that showed significant language differences are listed in this table, and the following are shown: *t*-value, original *t*-statistic; *P*, corrected *P*-value by permutation test; and Direction, the direction of comparison. L, left hemisphere; R, right hemisphere.

ROI analysis of network efficiency and local BOLD signal changes

To examine both the network efficiency and the regional activation patterns in the RN and the DMN during reading in the two languages, we performed ROI analyses on these two network modules. Fig. 4A displays the modular partition results of the AAL-90 template, in which 5 primary modules were identified (similar partition result for the AAL-1024 template). According to previous studies that were based on both seed-based functional connectivity analysis and independent component analysis (Koyama et al., 2010; Raichle, 2010; Tomasi and Volkow, 2012), these modules were consistently activated or deactivated, respectively, during cognitive tasks, and had dense intrinsic intra-modular connections. Thus, we labeled these 5 modules as "Reading", "Default-mode", "Sensorimotor", "Limbic", and "Visual".

Fig. 4B displays the bar charts of three brain measures (E_{glob}, E_{loc}, and *BOLD* signal change [effect size of Reading minus Rest]) for the two languages in both the DMN and RN modules. A double dissociation between E_{glob} and E_{loc} was observed in RN and DMN. We observed significantly increased E_{glob} for L1 in the RN ($t_{(1,39)} = 4.46$, $P = .00008$), but a non-significant language difference in the DMN ($t_{(1,39)} = 1.65$, $P = .11$) (Fig. 4B, top). In contrast, we found significantly increased E_{loc} for L2 in the DMN ($t_{(1,39)} = 4.49$, $P = .00004$) but no significant language difference in the RN ($t_{(1,39)} = 0.49$, $P = .62$; Fig. 4B middle). For the local *BOLD* signal change (Fig. 4C bottom), in both languages we found that there was activation in the RN, while there was deactivation in the DMN. Furthermore, we found greater activation in the RN ($t_{(1,39)} = 2.71$, $P = .0093$) but less deactivation in the DMN, ($t_{(1,39)} = 3.30$, $P = .0022$) when comparing L1 with L2 reading.

Correlation between network efficiency and local BOLD signal changes

Across the whole brain, strong association between the local *BOLD* signal changes and the network efficiency was found in both languages.

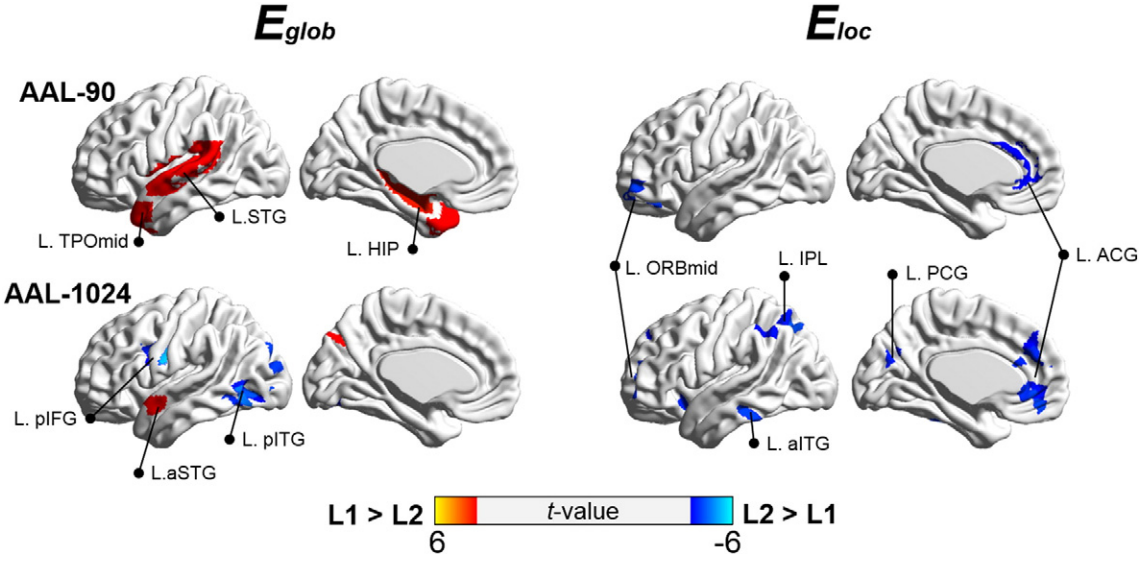

Fig. 3. Regions showing significantly increased (warm color) and decreased (cold color) regional AUC of E_{glob} and E_{loc}, in both AAL-90 (upper panel) and AAL-1024 templates (lower panel), respectively, during reading in L1 as compared with in L2. This figure is visualized on the standard rendered cortex surface by the BrainNet Viewer (Xia et al., 2013). All regions displayed here were significant at the corrected threshold of $P < .05$ (permutation test).

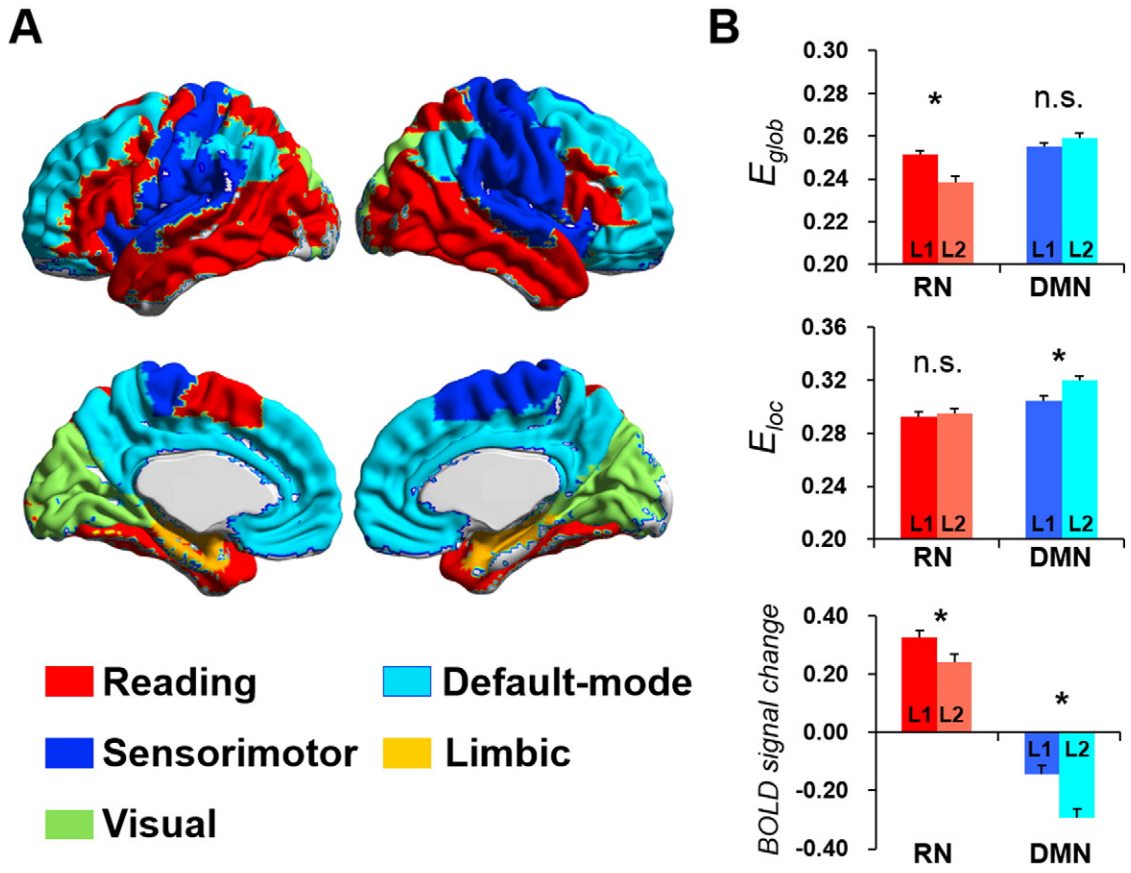

Fig. 4. Language differences in both functional network efficiency measures and local brain activation on both RN and DMN modules. A, Modular partition of group-level graphs based on the AAL-90 template. Whole-brain graphs were partitioned into five network modules by the Louvain algorithm (see Materials and methods section for details). B, ROI analysis of both RN and DMN modules on E_{glob}, E_{loc}, and local *BOLD* signal changes evoked by reading. Three bar-plots show the mean AUC of E_{glob} (top), E_{loc} (middle), and local *BOLD* signal changes (the effect size of the Reading condition minus the Rest condition, bottom) in each module and each language condition. Bars labeled with language condition: L1, Chinese; L2, English. Error bars indicated standard error of the mean. * $P < .01$, permutation test.

Regions with greater activation during reading tended to have higher network efficiency. Moreover, regions with greater deactivation also tended to have higher E_{glob} but such association was weaker for E_{loc} (Fig. 5 scatter plots) in both languages. A similar association was also found between local activation and the number of connections (*degree*). In addition, such *BOLD-Efficiency* relationship was slightly more prominent for L2 than L1 reading.

At the nodal level, regions exhibiting a significant positive *BOLD*-E_{glob} correlation were located in RN, whereas regions exhibiting a significant negative *BOLD*-E_{glob} correlation were located in DMN. These regions can be further separated into two groups. One group of regions showed language-common activation-efficiency correlations, and the other group of regions showed language-modulated correlation patterns (Fig. 6). The regions with language-common positive *BOLD*-E_{glob} correlations were mainly located in the left inferior frontal gyrus (IFGoperc and IFGtriang), right middle temporal cortex, and bilateral visual cortex. In contrast, regions with language-common negative *BOLD*-E_{glob} correlations were located in the left posterior cingulate gyrus, right angular gyrus, and right inferior parietal lobule. For the *BOLD*-E_{loc} correlation, no regions remained after FDR corrections. Thus, we used an uncorrected threshold of $P = .005$, which allowed us to identify language-common positive *BOLD*-E_{loc} correlated regions located in the left inferior frontal gyrus (L.IFGtriang), left precentral gyrus, right middle temple gyrus and right fusiform gyrus. The language-common negatively correlated regions were located in the left posterior cingulate gyrus.

In addition to the regions exhibiting common activation-efficiency correlation effects across languages, we also identified regions showing language-modulated activation-efficiency correlations (Fig. 6, purple regions). For example, the left middle temporal gyrus and the left superior medial frontal gyrus exhibited a significant *BOLD*-E_{glob} correlation in L2 but a much weaker correlation in L1. Similarly, we also observed language-modulated *BOLD*-E_{loc} correlations in several frontal and parietal regions, including the left inferior frontal gyrus, left supplemental motor areas and DMN regions in the right hemisphere (see detailed regions in Table 6).

Functional relationship between RN and DMN

To further investigate how the functional interactions between RN and DMN were associated with better reading performance, we performed correlation analyses between RN and DMN on local brain activation as well as E_{glob}. A dynamic relationship between the two networks on these measures is displayed in Fig. 7. We observed a significant positive correlation between L2 reading performance and RN activation but not for L1 reading, which might be due to the participants' reading performance reaching the ceiling. Underlying L2's performance-activation correlation, a competitive relationship between the two networks were observed. Individual differences in both RN activation and RN E_{glob} were negatively associated with individual differences in both DMN activation and DMN E_{glob} during reading in both languages, suggesting that fewer connections in DMN regions are associated with

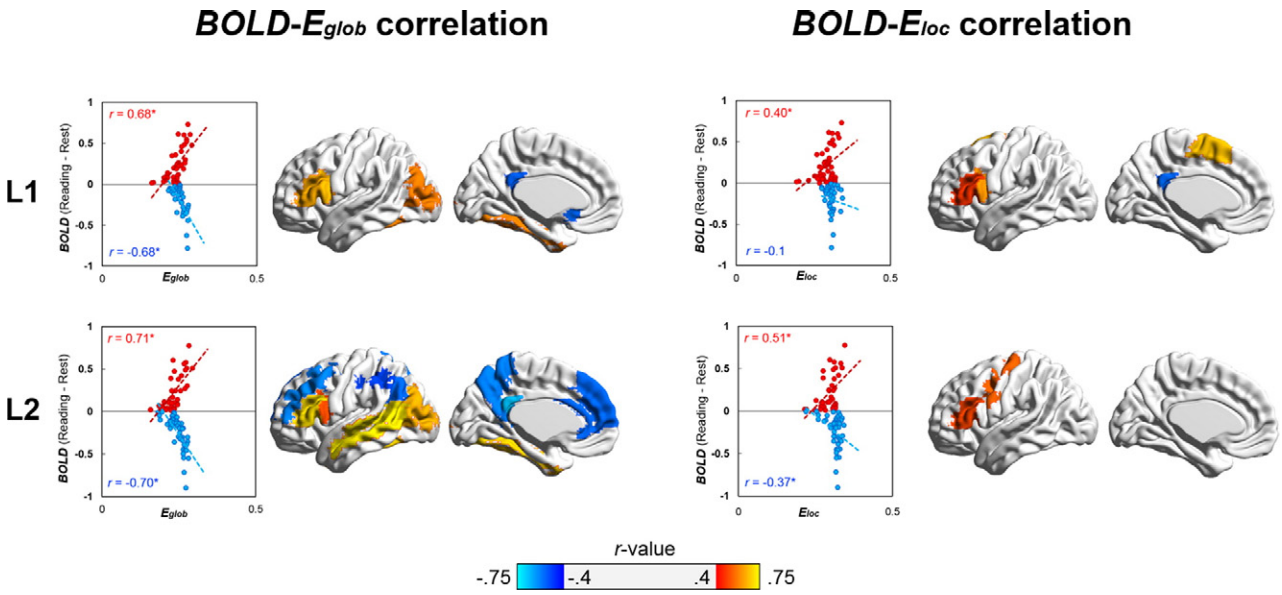

Fig. 5. Association between local brain activation and network efficiency (i.e., *BOLD-E_{glob}* correlation and *BOLD-E_{loc}* correlation) during reading in L1 and L2. The scatter plots show linear relationships between local brain activation and network efficiency. Each region in the template is represented by a small circle in the scatter plot. Red circles refer to activated regions, while blue circles refer to deactivated regions during reading. More activated and deactivated regions were tended to possess higher network efficiency. This effect was more salient during L2 reading. The brain maps show specific regions possessing significantly correlation between local brain activation and network efficiency. We focused on regions within the RN and the DMN modules defined by group-level partition. Regions displayed in a warm color exhibited significant positive *BOLD-Efficiency* correlations, whereas regions displayed in a cold color exhibited significant negative *BOLD-Efficiency* correlations. *BOLD-E_{glob}* correlations are used FDR corrected threshold at $P < .05$. However, no regions remained after multiple comparison correction on *BOLD-E_{loc}* correlation in both languages. Thus, regions that showed uncorrected $P < .005$ are displayed here for visualization.

more connections and greater activation in RN regions, which is associated with better L2 reading performance.

Discussion

Three main findings were observed. First, while greater activation was found in the RN regions during L1 reading, greater deactivation was observed in the DMN regions during L2 reading. Second, efficient L1 reading was associated with increased global network efficiency and decreased clustering, with the most significant differences in the temporal RN and medial prefrontal DMN regions. Finally, nodal network efficiency measures were closely associated with local brain activation, and such associations were also modulated by reading efficiency in the two languages. Our results demonstrate that a more economical, integrative and efficient brain network topology is associated with efficient reading, and further reveal a dynamic relationship between network efficiency and local activation for both RN and DMN during reading.

Local brain activation

We found greater activation in bilateral temporal cortices in L1 than in L2 reading. These observations converge with previous findings reporting enhanced brain activation in temporal regions during L1 processing, using both PET (Perani et al., 1996) and fMRI (Ruschemeyer et al., 2005). Our findings are also consistent with previous reports that greater activation in the middle temporal regions is associated with better reading ability (Meyler et al., 2007), while underactivation in these regions has been found in dyslexic children (Shaywitz et al., 1998). Our data further revealed greater deactivation in DMN regions, including superior frontal gyrus and bilateral supramarginal gyrus, in L2 than in L1 reading. That previous studies did not report these deactivated regions might be due to either the use of different baselines or differences between imaging techniques (PET vs. fMRI).

Additionally, L2 reading induced greater activation in the left posterior inferior frontal gyrus (LIFG) and the left inferior temporal gyrus (LITG). This is consistent with previous observations that less proficient bilinguals recruit additional frontal regions and low-level reading-related regions (Nakamura et al., 2010; Perani and Abutalebi, 2005), which may be related to the increased cognitive efforts required for L2 processing (Green, 1998).

Functional network efficiency

An increasing number of studies have reported that similar cortical areas are recruited across languages in a variety of tasks. Consistent with and further extending these observations, we found that the modular structures of the functional networks were not significantly different between L1 and L2 reading (see Table 4, modularity Q). As modular structures measure the underlying recruited network organization, this result suggests that reading in the two languages recruits not only similar brain areas but also similar functional network modularity, even if L2 is acquired after the critical period. In line with this finding, previous study has found that functional network modularity was similar across different age groups although they differed in their reading performance (Vogel et al., 2013). The fact that the two languages recruit the same brain network provides a chance to compare network efficiency in RN and DMN across languages.

We found a more globally efficient but less clustered functional network topology during L1 reading than during L2 reading, which is consistent with our prediction that a more optimized functional network organization emerges during L1 processing. These results suggest that a smaller number of intermediate steps in the information integration pathway, resulting from increased global connections with decreased local connections, may reflect more accurate and rapid neural communications during native language reading. Such a tradeoff between global integration and local specialization is consistent with previous findings, in which better task performance was associated

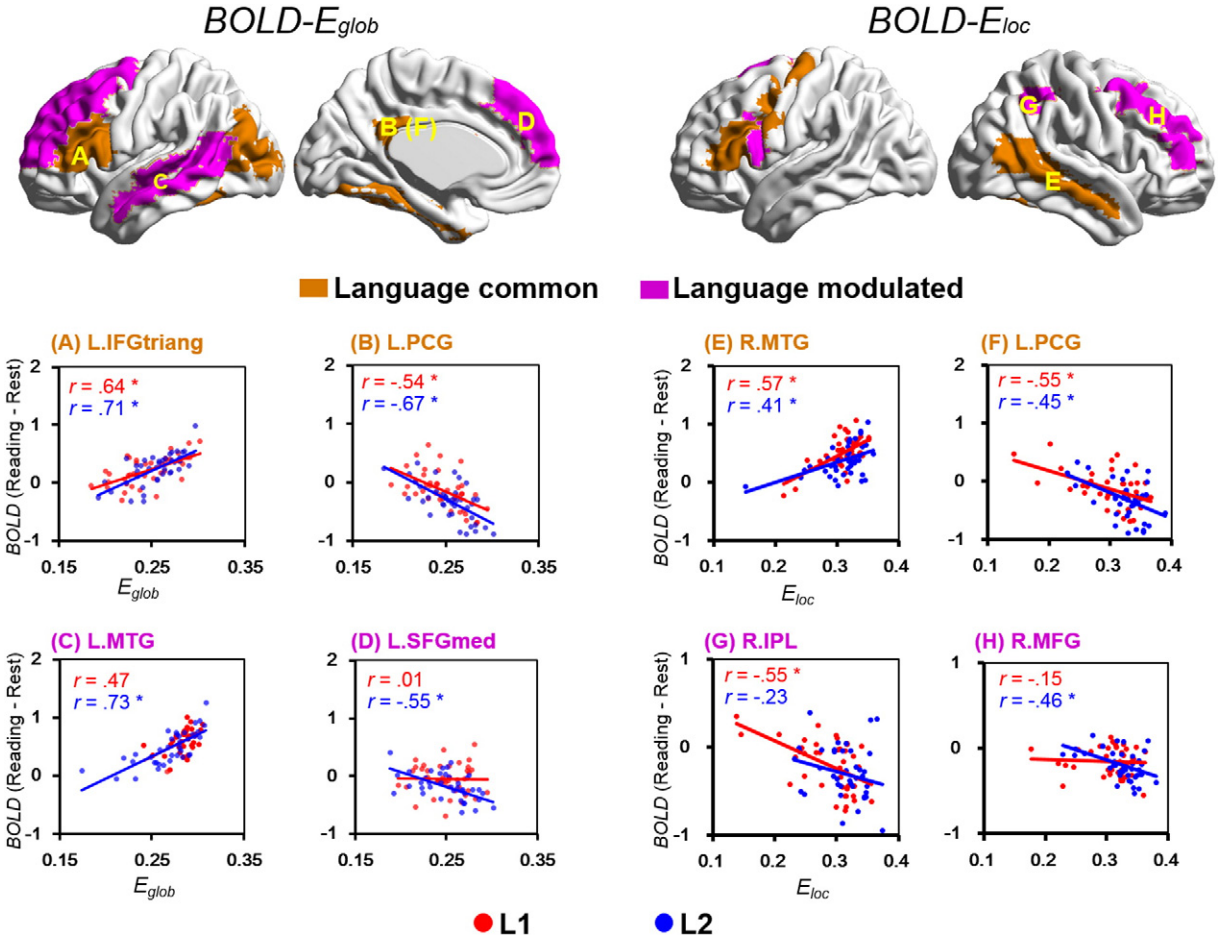

Fig. 6. Regions showing language-common and language-modulated *BOLD-E_{glob}* and *BOLD-E_{loc}* correlation. The regions in brown are represented as language-common *BOLD-Efficiency* correlation, while the regions in purple are represented as language-modulated *BOLD-Efficiency* correlation. Lower panel, A–D, Scatter plots with linear regression slopes for four regions with representative language-common (L.IFGtriang and L.PCG) and language-modulated (L.MTG and L.SFGmed) effects on *BOLD-E_{glob}* correlation are presented. E–F, Scatter plots with representative language-common (R.MTG and L.PCG) and language-modulated (R.IPL and R.MFG) effects on *BOLD-E_{loc}* correlation are also presented (for other regions with similar patterns, refer to Table 6). In all scatter plots, the *y*-axis shows activation amplitude as effect size of the Reading relative to the Rest condition. * in the scatter plots of *BOLD-E_{glob}* correlation denotes $P < 0.05$ (FDR corrected); * for *BOLD-E_{loc}* correlation denotes $P < 0.005$ (uncorrected).

Table 6
Regions that showed common and modulated *BOLD-E_{glob}* correlation and *BOLD-E_{loc}* correlation in the two languages.

***BOLD-E_{glob}* correlation**			***BOLD-E_{loc}* correlation**		
Regions	*r*-value (L1)	*r*-value (L2)	Regions	*r*-value (L1)	*r*-value (L2)
Language-common					
L. IFGoperc	0.66	0.51	L. IFGtriang	0.48	0.50
L. IFGtriang	0.64	0.71	L. PreCG	0.41	0.54
L. FFG	0.59	0.70	R. MTG	0.57	0.41
L. MOG	0.58	0.65	R. FFG	0.58	0.45
R. MTG	0.71	0.62	L. PCG	−0.55	−0.45
R. FFG	0.65	0.70			
R. MOG	0.73	0.79			
L. PCG	−0.54	−0.67			
R. ANG	−0.53	−0.49			
R. IPL	−0.60	−0.55			
Language-modulated					
R. ORBsup	−0.52*	0.03	L. IFGoperc	0.61*	0.35
L. MTG	0.47	0.73*	L. SMA	0.67*	0.34
L. SFGmed	0.01	−0.55*	R. PCG	−0.61*	−0.19
L. SFGdor	−0.12	−0.45*	R. IPL	−0.55*	−0.23
L. MFG	−0.26	−0.59*	R. MFG	−0.15	−0.46*
R. ACG	−0.37	−0.63*			

Regions that showed no significantly different *BOLD-E_{glob}* correlation (or *BOLD-E_{loc}* correlation) between L1 and L2 (but showed significance in both languages) were considered as language-common regions; while regions that showed significantly different *BOLD-E_{glob}* correlation (or *BOLD-E_{loc}* correlation) between the two languages were considered as language-modulated regions (* $P < 0.05$, FDR corrected).

with a more integrated brain network with less clustered topological organization (Giessing et al., 2013; Kitzbichler et al., 2011; Sheppard et al., 2012).

Moreover, the network we observed had increased maximal cost-efficiency in L1 reading, which indicates a more economical balance between global efficiency and connection cost (Kaiser, 2011; Sporns, 2011). Such economic network organization, with low-cost and efficient coordination of multiple reading-related regions, may be associated with L1's relatively automatic and accurate reading processing (Friederici, 2012). On the one hand, this increased cost-efficiency during L1 narrative reading could be a consequence of long-term language training or L1's extensive usage. On the other hand, the slow process of learning a language might change the brain network organization gradually (Bialystok et al., 2012), resulting in an organization optimal for supporting the processing of specific language stimuli. This idea is supported by previous studies reporting that learning a second language modulated bilinguals' functional brain activity and anatomical brain volume (Mechelli et al., 2004; Rodriguez-Fornells et al., 2002). Moreover, anomalous functional connectivity was found between the left hemisphere reading-related regions in patients with developmental dyslexia (Schurz et al., 2014). Altogether, these findings suggest that even though the processing of L1 and a non-efficient L2 share similar brain language systems, the efficiency of processing a language is associated with functional network topology.

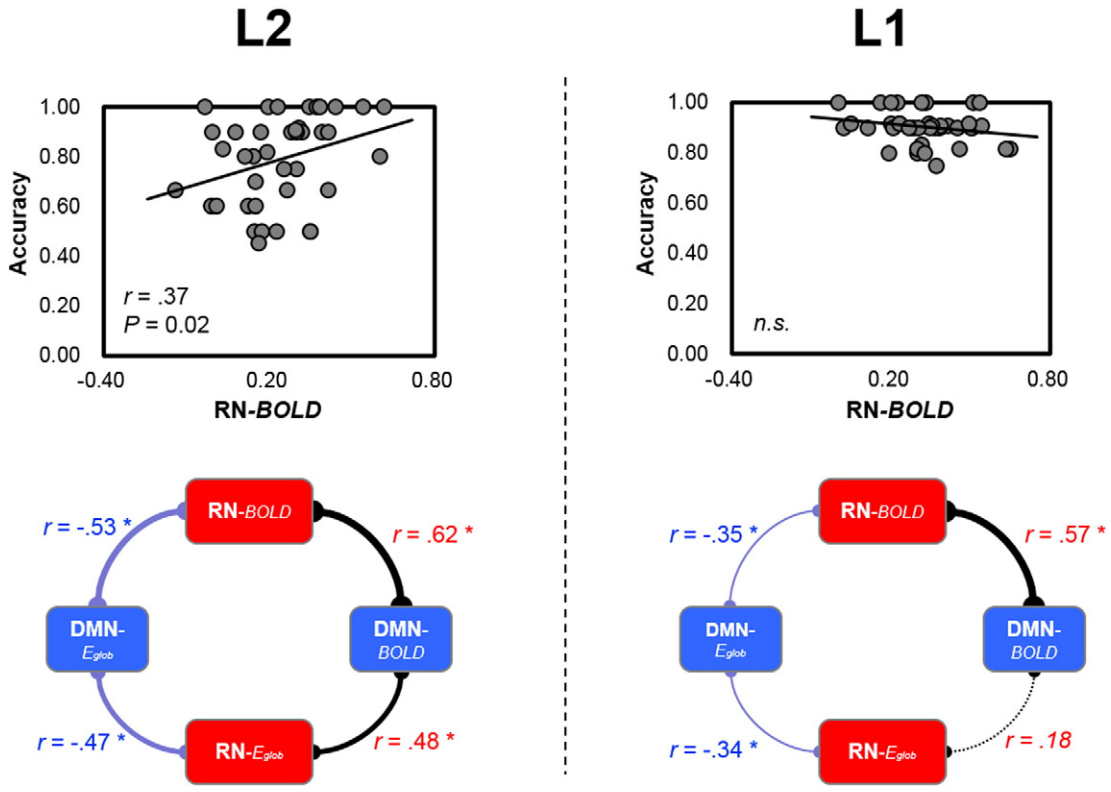

Fig. 7. Correlation between RN and DMN on both local *BOLD* signal changes as well as E_{glob} druing reading in the two languages. In the L2 reading, both decreased network efficiency and increased local activation in DMN associated with increased E_{glob} and local activation in RN, which the later is associated with better behavioral performance. Similar relationship was found in the L1 reading. The blue boxes refer to DMN, while the red boxes refer to RN. Light blue links among networks represent negative correlation, while the black links represent positive correlation. * $P < 0.05$.

Association between local activation and network efficiency: RN vs. DMN

The current consensus holds that both activity in local regions and connectivity across regions are associated with high-level cognitive functions, such as language comprehension. However, it is still largely unknown how the local brain activation is associated with this network connectivity organization, and how such an association is linked with efficient reading. In the present study, we have provided evidence to show that there is a close association between local activation and network organization (i.e., network efficiency), and that the dynamics of this association are linked with reading efficiency.

First, our data not only showed that the RN module (including bilateral fronto-temporal regions and visual cortices) had both enhanced local activation and increased global network efficiency during L1 reading, but also revealed that individual differences in local activity were positively correlated with individual differences in global network efficiency within the RN. These associations were prominent for the *BOLD*-E_{glob} in both languages, reflecting regions more activated in the reading task recruited more global connections but relatively fewer local connections. This strong link is consistent with previous observations that these RN regions are co-activated during various language tasks, and are associated with multiple language and memory processes: the left middle/superior temporal cortex is associated with semantic processing both at word and sentence levels (Friederici, 2011; Price, 2010), while the recruitment of its right-hemisphere counterpart is associated with discourse-level processes necessary for building coherence (Perfetti and Frishkoff, 2008), or coarse computation of semantic information (Jung-Beeman, 2005). In light of these previous findings, our results show that enhanced local brain response is linked with increased global network efficiency for these RN regions, which may facilitate the processing of linguistic information at multiple levels.

As mentioned earlier, the RN consists of several regions that are nodes of the fronto-parietal control network (Vincent et al., 2008) and the dorsal-attention network (Fox et al., 2006). These two networks are known to be associated with general cognitive control and attention processing, respectively. Since reading is a complex process that also requires general cognitive control (Fedorenko and Thompson-Schill, 2014), as compared with other baseline control tasks, the reading process could lead to increasing activations within these networks as well as more connections between these and other reading-related regions (Cole et al., 2013; Lohmann et al., 2010; Vogel et al., 2012a). Indeed, previous studies suggested that although the regions we referred to here as RN could be implicated during reading, they are not intrinsically specified for reading (Vogel et al., 2013). The recruitment of these regions may be the consequence of a general mechanism of cognitive control. More specifically, it is possible that the association between the local activation and network efficiency uncovered here could be attributed to a more efficient use of a generally activated cognitive control network, instead of a reading network *per se*. An account that appeals to such domain general networks makes further predictions that the more efficient use of a cognitive control network should not only lead to better reading performance, but also to better behavioral performance in other cognitive domains. Future studies are needed to address such possibility (for evidence supporting this hypothesis, see Cole et al., 2013).

In contrast to the above-mentioned RN regions, two regions (posterior LIFG and posterior LITG) within the RN exhibited both enhanced brain response and increased global network efficiency in L2 reading.

Posterior LIFG (close to the precentral gyrus) is frequently associated with cognitive control (Badre et al., 2005; Gold et al., 2006; Zhu et al., 2013), whereas LITG is involved in visual word form processing (Dehaene et al., 2010; Price and Devlin, 2011). Both regions have rich input and output connections uncovered using fiber tracking (Ben-Shachar et al., 2007; Saur et al., 2008) and resting-state functional connectivity (Tomasi and Volkow, 2012; Xiang et al., 2010). Previous studies have shown that the response of LITG in word recognition is modulated by top-down signals from inferior frontal regions (Mano et al., 2013). Consistent with this perspective, our findings suggest that LIFG and LITG may be communicating with each other, especially during reading of the relatively unfamiliar L2. In addition to the control effort account for LIFG, an alternative explanation is that LIFG may be more involved in linguistic computation during L2 reading (Tatsuno and Sakai, 2005). Previous studies have suggested that LIFG is associated with morphology, syntax, retrieval of lexical entries and phonological processing (Friederici, 2011; Hagoort, 2005). Greater activation and increased global network efficiency in both the LIFG and the LITG may reflect that both word form analysis and phonological processing are more taxing during L2 reading as compared with that in L1.

Second, regions in the DMN, including the bilateral medial prefrontal cortex, posterior cingulate gyrus, and bilateral inferior parietal regions, exhibited greater deactivation and increased clustering in L2 reading. These regions also showed a significant negative activation-efficiency correlation in both language conditions. The DMN has been proposed to be associated with monitoring external stimuli and allocating cognitive resources (Chadick and Gazzaley, 2011; Spreng, 2012). Suppression of DMN activity may play a critical role in inhibiting internal self-referential processing and consequently facilitating stimulus-driven information processing (Anticevic et al., 2012; McKiernan et al., 2003; Wen et al., 2013). For instance, successful DMN suppression has been shown to be associated with better performance in variety of tasks (Anticevic et al., 2010; Daselaar et al., 2004). Consistent with and extending these previous findings, robust negative *BOLD-E_{glob}* correlations in the DMN regions indicate that DMN suppression is important to efficient global information communication during reading comprehension.

In addition to the regions exhibiting similar activation–efficiency correlations across languages, we also identified regions that showed significantly different activation–efficiency relationships in L1 and L2 reading. In particular, the left middle temporal gyrus (LMTG) and medial prefrontal cortex both showed stronger *BOLD-E_{glob}* correlations in L2 than in L1 reading. A recent study has shown that spontaneous LMTG activity is highly correlated with participants' semantic processing efficiency (Wei et al., 2012). Considering the importance of LMTG in semantic processing, it is possible that both enhanced regional activity and increased connectivity of the LMTG with other brain regions improve conceptual-level processing during narrative reading, which is associated with more efficient reading processing (i.e., L1 > L2). Moreover, several regions exhibiting such language-modulated *BOLD-E_{loc}* correlation effects were observed in the fronto-motor circuit and the PCG-IPL circuit within the DMN. All these observations indicate that the activation–efficiency correlations for RN and DMN regions are modulated by the language reading efficiency.

Finally, the RN and DMN showed a competitive relationship in both local brain activation and functional network efficiency. Individual variability of both local activation and network efficiency in RN were negatively correlated with network efficiency in DMN, which suggests that reduced connection of the DMN regions (less global network efficiency in DMN) is associated with both increased connections and enhanced local brain activation in the RN regions. Such a relationship was observed during reading in both languages but was more significant in L2, because the participants' L2 proficiency spanned a wide range while that of L1 was close to the ceiling. Furthermore, the individual variability of local activation in RN was correlated with reading performance during reading in the underdeveloped L2. The correlation of reduced connections among DMN regions with increased connections among RN regions may reflect the fact that the minimization of interfering neural processes in the DMN regions and maximization of reading-related neural communication underlie efficient reading.

Conclusion

The present study revealed a more efficient network organization supporting fast and automatic L1 reading, and identified a strong link between local activity and network efficiency. Specifically, in the RN, enhanced local activity was associated with increased network efficiency, whereas in the DMN, greater deactivation was accompanied by the increase in global communication efficiency. This close relationship appears to be strongly relevant for efficient and automatic reading. The results underscore the importance to consider interregional connectivity when interpreting local signal changes in bilingual reading. Furthermore, the relationship between local activation and global network communication could be used as an effective index of language learning progress or investigating mechanisms of language disorders (e.g., aphasia and dyslexia).

Supplementary data to this article can be found online at http://dx.doi.org/10.1016/j.neuroimage.2015.05.100.

Acknowledgments

This work was funded by grants from the Natural Science Foundation of China (31271086), and key project from the Natural Science Foundation of Guangdong Province, China (2014A030311016) to Suiping Wang, and by grants from the Research Grants Council of the Hong Kong Special Administrative Region, China (CUHK441008 and 441811) to Hsuan-Chih Chen. We thank Zhizhou Deng for his assistance with fMRI data collection and Zhengjia Dai for her help with data analysis, and William F. Broderick for his helpful language editing of our earlier version of the manuscript. We also thank Olaf Sporns and Mikail Rubinov for sharing Matlab functions in their freely available Brain Connectivity Toolbox, which we implemented together with in-house scripts to carry out the analyses.

Conflict of interest

The authors declare no conflict of interest.

Appendix A

Table A1
Six whole-brain network metrics were calculated during the resting-state (prior to the reading task) and the L1/L2 reading task.

Metrics	L1	L2	*Resting-state*	Direction
E_{glob}	0.243 (0.006)	0.239 (0.009)	0.249 (0.003)	Rest > L1 > L2
E_{loc}	0.296 (0.007)	0.298 (0.006)	0.295 (0.005)	L2 > L1 ≈ Rest
CE_{max}	0.346 (0.017)	0.335 (0.021)	0.361 (0.010)	Rest > L1 > L2
L_p	0.685 (0.031)	0.705 (0.045)	0.659 (0.010)	Rest < L1 < L2
C_p	0.222 (0.014)	0.230 (0.014)	0.212 (0.011)	L2 > L1 > Rest
Modularity *Q*	0.184 (0.011)	0.187 (0.010)	0.188 (0.017)	L1 ≈ L2 < Rest

Note. "<" and ">" represent significant differences between conditions. "≈" represents none significant difference. The threshold used is $P < 0.05$ after correcting for multiple comparisons.

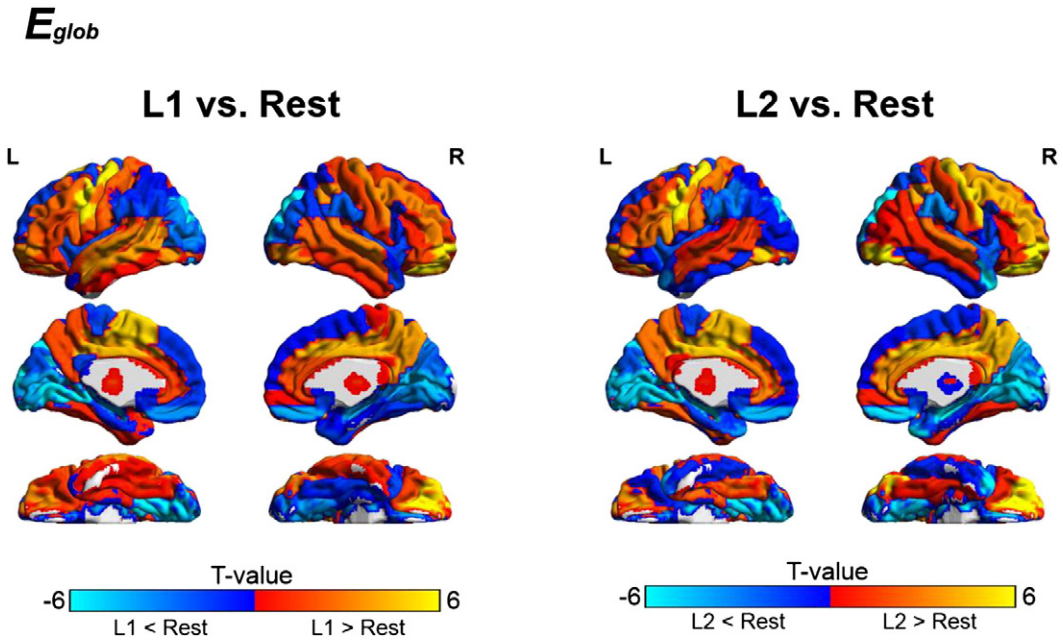

Fig. A1. The global network efficiency differences between L1 reading and the true resting-state (L1 vs. Rest), and differences between L2 reading and the resting-state (L2 vs. Rest). Whole brain uncorrected contrast maps were presented using AAL90 template. L, left hemisphere; R, right hemisphere. Warm-color areas represented regions showing increased global efficiency during reading (most of them were the reading-related regions), while cool-color areas represented regions showing increased global efficiency during resting-state (most of them located within the default-mode network).

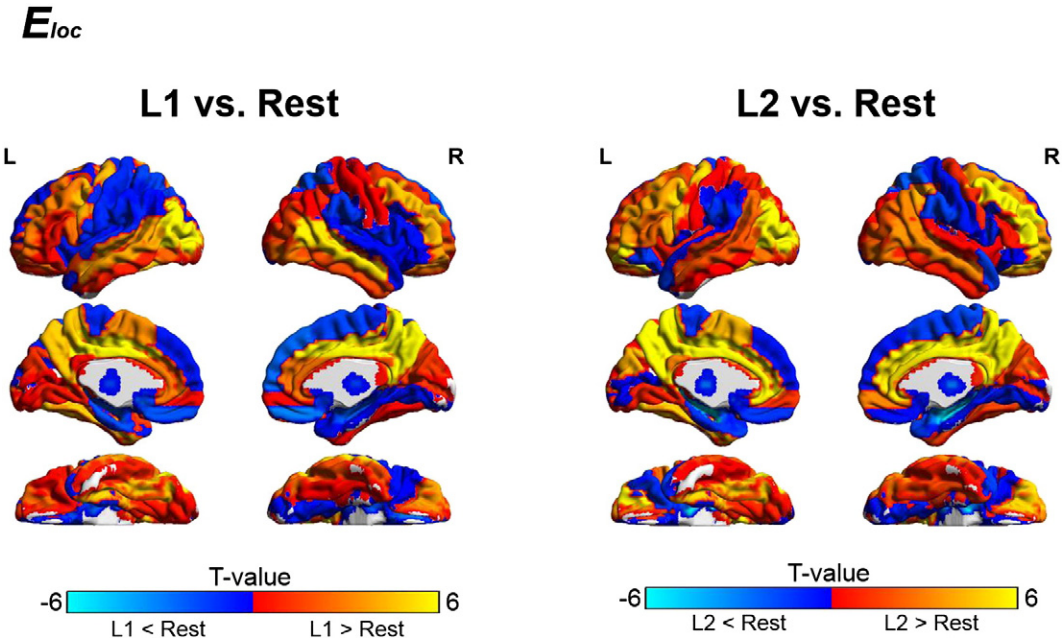

Fig. A2. The local network efficiency differences between L1 reading and the true resting-state (L1 vs. Rest), and differences between L2 reading and the resting-state (L2 vs. Rest). Whole-brain uncorrected contrast maps were presented by using the AAL90 template. L, left hemisphere; R, right hemisphere.

References

Abutalebi, J., 2008. Neural aspects of second language representation and language control. Acta Psychol. 128, 466–478.

Achard, S., Bullmore, E.T., 2007. Efficiency and cost of economical brain functional networks. PLoS Comput. Biol. 3, e17.

Anticevic, A., Repovs, G., Shulman, G.L., Barch, D.M., 2010. When less is more: TPJ and default network deactivation during encoding predicts working memory performance. NeuroImage 49, 2638–2648.

Anticevic, A., Cole, M.W., Murray, J.D., Corlett, P.R., Wang, X.J., Krystal, J.H., 2012. The role of default network deactivation in cognition and disease. Trends Cogn. Sci. 16, 584–592.

Badre, D., Poldrack, R.A., Paré-Blagoev, E.J., Insler, R.Z., Wagner, A.D., 2005. Dissociable controlled retrieval and generalized selection mechanisms in ventrolateral prefrontal cortex. Neuron 47, 907–918.

Ben-Shachar, M., Dougherty, R.F., Wandell, B.A., 2007. White matter pathways in reading. Curr. Opin. Neurobiol. 17, 258–270.

Bialystok, E., Craik, F.I., Luk, G., 2012. Bilingualism: consequences for mind and brain. Trends Cogn. Sci. 16, 240–250.

Binder, J.R., Desai, R.H., Graves, W.W., Conant, L.L., 2009. Where is the semantic system? A critical review and meta-analysis of 120 functional neuroimaging studies. Cereb. Cortex 19, 2767–2796.

Blondel, V.D., Guillaume, J.L., Lambiotte, R., Lefebvre, E., 2008. Fast unfolding of communities in large networks. J. Stat. Mech: Theory Exp. 2008, P10008.

Bullmore, E.T., Bassett, D.S., 2011. Brain graphs: graphical models of the human brain connectome. Annu. Rev. Clin. Psychol. 7, 113–140.
Bullmore, E.T., Sporns, O., 2009. Complex brain networks: graph theoretical analysis of structural and functional systems. Nat. Rev. Neurosci. 10, 186–198.
Bullmore, E.T., Sporns, O., 2012. The economy of brain network organization. Nat. Rev. Neurosci. 13, 336–349.
Chadick, J.Z., Gazzaley, A., 2011. Differential coupling of visual cortex with default or frontal-parietal network based on goals. Nat. Neurosci. 14, 830–832.
Chee, M.W.L., Caplan, D., Soon, C.S., Sriram, N., Tan, E.W., Thiel, T., Weekes, B., 1999a. Processing of visually presented sentences in Mandarin and English studied with fMRI. Neuron 23, 127–137.
Chee, M.W.L., Tan, E.W., Thiel, T., 1999b. Mandarin and English single word processing studied with functional magnetic resonance imaging. J. Neurosci. 19, 3050–3056.
Chee, M.W.L., Weekes, B., Lee, K.M., Soon, C.S., Schreiber, A., Hoon, J.J., Chee, M., 2000. Overlap and dissociation of semantic processing of Chinese characters, English words, and pictures: evidence from fMRI. NeuroImage 12, 392–403.
Cole, M.W., Reynolds, J.R., Power, J.D., Repovs, G., Anticevic, A., Braver, T.S., 2013. Multi-task connectivity reveals flexible hubs for adaptive task control. Nat. Neurosci. 16, 1348–1355.
Cordes, D., Haughton, V.M., Arfanakis, K., Carew, J.D., Turski, P.A., Moritz, C.H., Quigley, M.A., Meyerand, M.E., 2001. Frequencies contributing to functional connectivity in the cerebral cortex in "resting-state" data. AJNR Am. J. Neuroradiol. 22, 1326–1333.
Crossley, N.A., Mechelli, A., Vertes, P.E., Winton-Brown, T.T., Patel, A.X., Ginestet, C.E., McGuire, P., Bullmore, E.T., 2013. Cognitive relevance of the community structure of the human brain functional coactivation network. Proc. Natl. Acad. Sci. U. S. A. 110, 11583–11588.
Daselaar, S.M., Prince, S.E., Cabeza, R., 2004. When less means more: deactivations during encoding that predict subsequent memory. NeuroImage 23, 921–927.
Dehaene, S., Pegado, F., Braga, L.W., Ventura, P., Nunes Filho, G., Jobert, A., Dehaene-Lambertz, G., Kolinsky, R., Morais, J., Cohen, L., 2010. How learning to read changes the cortical networks for vision and language. Science 330, 1359–1364.
Elston-Güttler, K.E., Gunter, T.C., Kotz, S.A., 2005. Zooming into L2: global language context and adjustment affect processing of interlingual homographs in sentences. Cogn. Brain Res. 25, 57–70.
Fair, D.A., Schlaggar, B.L., Cohen, A.L., Miezin, F.M., Dosenbach, N.U., Wenger, K.K., Fox, M.D., Snyder, A.Z., Raichle, M.E., Petersen, S.E., 2007. A method for using blocked and event-related fMRI data to study "resting state" functional connectivity. NeuroImage 35, 396–405.
Fedorenko, E., Thompson-Schill, S.L., 2014. Reworking the language network. Trends Cogn. Sci. 18, 120–126.
Fornito, A., Zalesky, A., Bullmore, E.T., 2010. Network scaling effects in graph analytic studies of human resting-state FMRI data. Front. Syst. Neurosci. 4, 22.
Fornito, A., Zalesky, A., Bassett, D.S., Meunier, D., Ellison-Wright, I., Yucel, M., Wood, S.J., Shaw, K., O'Connor, J., Nertney, D., Mowry, B.J., Pantelis, C., Bullmore, E.T., 2011. Genetic influences on cost-efficient organization of human cortical functional networks. J. Neurosci. 31, 3261–3270.
Fortunato, S., 2010. Community detection in graphs. Phys. Rep. Rev. Sect. Phys. Lett. 486, 75–174.
Fox, M.D., Snyder, A.Z., Vincent, J.L., Corbetta, M., Van Essen, D.C., Raichle, M.E., 2005. The human brain is intrinsically organized into dynamic, anticorrelated functional networks. Proc. Natl. Acad. Sci. U. S. A. 102, 9673–9678.
Fox, M.D., Corbetta, M., Snyder, A.Z., Vincent, J.L., Raichle, M.E., 2006. Spontaneous neuronal activity distinguishes human dorsal and ventral attention systems. Proc. Natl. Acad. Sci. U. S. A. 103, 10046–10051.
Friederici, A.D., 2011. The brain basis of language processing: from structure to function. Physiol. Rev. 91, 1357–1392.
Friederici, A.D., 2012. The cortical language circuit: from auditory perception to sentence comprehension. Trends Cogn. Sci. 16, 262–268.
Friederici, A.D., Gierhan, S.M., 2013. The language network. Curr. Opin. Neurobiol. 23, 250–254.
Genovese, C.R., Lazar, N.A., Nichols, T., 2002. Thresholding of statistical maps in functional neuroimaging using the false discovery rate. NeuroImage 15, 870–878.
Giessing, C., Thiel, C.M., Alexander-Bloch, A.F., Patel, A.X., Bullmore, E.T., 2013. Human brain functional network changes associated with enhanced and impaired attentional task performance. J. Neurosci. 33, 5903–5914.
Gold, B.T., Balota, D.A., Jones, S.J., Powell, D.K., Smith, C.D., Andersen, A.H., 2006. Dissociation of automatic and strategic lexical-semantics: functional magnetic resonance imaging evidence for differing roles of multiple frontotemporal regions. J. Neurosci. 26, 6523–6532.
Green, D.W., 1998. Mental control of the bilingual lexico-semantic system. Biling.: Lang. Cogn. 1, 67–81.
Greicius, M.D., Krasnow, B., Reiss, A.L., Menon, V., 2003. Functional connectivity in the resting brain: a network analysis of the default mode hypothesis. Proc. Natl. Acad. Sci. U. S. A. 100, 253–258.
Hagoort, P., 2005. On Broca, brain, and binding: a new framework. Trends Cogn. Sci. 9, 416–423.
Hayasaka, S., Laurienti, P.J., 2010. Comparison of characteristics between region- and voxel-based network analyses in resting-state fMRI data. NeuroImage 50, 499–508.
He, Y., Evans, A., 2010. Graph theoretical modeling of brain connectivity. Curr. Opin. Neurol. 23, 341–350.
He, Y., Wang, J., Wang, L., Chen, Z.J., Yan, C., Yang, H., Tang, H., Zhu, C., Gong, Q., Zang, Y., Evans, A.C., 2009. Uncovering intrinsic modular organization of spontaneous brain activity in humans. PLoS One 4, e5226.
Indefrey, P., 2006. A meta-analysis of hemodynamic studies on first and second language processing: which suggested differences can we trust and what do they mean? Lang. Learn. 56, 279–304.
Jia, Z., 2002. A Collection of English Readings. Tianjin University, Tianjin.
Jung-Beeman, M., 2005. Bilateral brain processes for comprehending natural language. Trends Cogn. Sci. 9, 512–518.
Kaiser, M., 2011. A tutorial in connectome analysis: topological and spatial features of brain networks. NeuroImage 57, 892–907.
Kitzbichler, M.G., Henson, R.N., Smith, M.L., Nathan, P.J., Bullmore, E.T., 2011. Cognitive effort drives workspace configuration of human brain functional networks. J. Neurosci. 31, 8259–8270.
Koyama, M.S., Kelly, C., Shehzad, Z., Penesetti, D., Castellanos, F.X., Milham, M.P., 2010. Reading networks at rest. Cereb. Cortex 20, 2549–2559.
Koyama, M.S., Di Martino, A., Zuo, X.N., Kelly, C., Mennes, M., Jutagir, D.R., Castellanos, F.X., Milham, M.P., 2011. Resting-state functional connectivity indexes reading competence in children and adults. J. Neurosci. 31, 8617–8624.
Laird, A.R., Fox, P.M., Eickhoff, S.B., Turner, J.A., Ray, K.L., McKay, D.R., Glahn, D.C., Beckmann, C.F., Smith, S.M., Fox, P.T., 2011. Behavioral interpretations of intrinsic connectivity networks. J. Cogn. Neurosci. 23, 4022–4037.
Latora, V., Marchiori, M., 2001. Efficient behavior of small-world networks. Phys. Rev. Lett. 87, 198701.
Lohmann, G., Hoehl, S., Brauer, J., Danielmeier, C., Bornkessel-Schlesewsky, I., Bahlmann, J., Turner, R., Friederici, A., 2010. Setting the frame: the human brain activates a basic low-frequency network for language processing. Cereb. Cortex 20, 1286–1292.
Mano, Q.R., Humphries, C., Desai, R.H., Seidenberg, M.S., Osmon, D.C., Stengel, B.C., Binder, J.R., 2013. The role of left occipitotemporal cortex in reading: reconciling stimulus, task, and lexicality effects. Cereb. Cortex 23, 988–1001.
McKiernan, K.A., Kaufman, J.N., Kucera-Thompson, J., Binder, J.R., 2003. A parametric manipulation of factors affecting task-induced deactivation in functional neuroimaging. J. Cogn. Neurosci. 15, 394–408.
Mechelli, A., Crinion, J.T., Noppeney, U., O'Doherty, J., Ashburner, J., Frackowiak, R.S., Price, C.J., 2004. Neurolinguistics: structural plasticity in the bilingual brain. Nature 431, 757.
Meyler, A., Keller, T.A., Cherkassky, V.L., Lee, D., Hoeft, F., Whitfield-Gabrieli, S., Gabrieli, J.D., Just, M.A., 2007. Brain activation during sentence comprehension among good and poor readers. Cereb. Cortex 17, 2780–2787.
Nakamura, K., Kouider, S., Makuuchi, M., Kuroki, C., Hanajima, R., Ugawa, Y., Ogawa, S., 2010. Neural control of cross-language asymmetry in the bilingual brain. Cereb. Cortex 20, 2244–2251.
Nakamura, K., Kuo, W.J., Pegado, F., Cohen, L., Tzeng, O.J., Dehaene, S., 2012. Universal brain systems for recognizing word shapes and handwriting gestures during reading. Proc. Natl. Acad. Sci. U. S. A. 109, 20762–20767.
Newman, M.E., 2006. Modularity and community structure in networks. Proc. Natl. Acad. Sci. U. S. A. 103, 8577–8582.
Nichols, T.E., Holmes, A.P., 2002. Nonparametric permutation tests for functional neuroimaging: a primer with examples. Hum. Brain Mapp. 15, 1–25.
Park, H.J., Friston, K., 2013. Structural and functional brain networks: from connections to cognition. Science 342, 1238411.
Perani, D., Abutalebi, J., 2005. The neural basis of first and second language processing. Curr. Opin. Neurobiol. 15, 202–206.
Perani, D., Dehaene, S., Grassi, F., Cohen, L., Cappa, S.F., Dupoux, E., Fazio, F., Mehler, J., 1996. Brain processing of native and foreign languages. Neuroreport 7, 2439–2444.
Perfetti, C.A., Frishkoff, G.A., 2008. The neural bases of text and discourse processing. Handbook of the Neuroscience of Language. Elsevier, San Diego, pp. 165–174.
Power, J.D., Cohen, A.L., Nelson, S.M., Wig, G.S., Barnes, K.A., Church, J.A., Vogel, A.C., Laumann, T.O., Miezin, F.M., Schlaggar, B.L., Petersen, S.E., 2011. Functional network organization of the human brain. Neuron 72, 665–678.
Price, C.J., 2010. The anatomy of language: a review of 100 fMRI studies published in 2009. Ann. N. Y. Acad. Sci. 1191, 62–88.
Price, C.J., Devlin, J.T., 2011. The interactive account of ventral occipitotemporal contributions to reading. Trends Cogn. Sci. 15, 246–253.
Raichle, M.E., 2010. Two views of brain function. Trends Cogn. Sci. 14, 180–190.
Raichle, M.E., MacLeod, A.M., Snyder, A.Z., Powers, W.J., Gusnard, D.A., Shulman, G.L., 2001. A default mode of brain function. Proc. Natl. Acad. Sci. U. S. A. 98, 676–682.
Rodriguez-Fornells, A., Rotte, M., Heinze, H.-J., Nosselt, T., Munte, T.F., 2002. Brain potential and functional MRI evidence for how to handle two languages with one brain. Nature 415, 1026–1029.
Ruschemeyer, S.A., Fiebach, C.J., Kempe, V., Friederici, A.D., 2005. Processing lexical semantic and syntactic information in first and second language: fMRI evidence from German and Russian. Hum. Brain Mapp. 25, 266–286.
Salmelin, R., Kujala, J., 2006. Neural representation of language: activation versus long-range connectivity. Trends Cogn. Sci. 10, 519–525.
Saur, D., Kreher, B.W., Schnell, S., Kummerer, D., Kellmeyer, P., Vry, M.S., Umarova, R., Musso, M., Glauche, V., Abel, S., Huber, W., Rijntjes, M., Hennig, J., Weiller, C., 2008. Ventral and dorsal pathways for language. Proc. Natl. Acad. Sci. U. S. A. 105, 18035–18040.
Schurz, M., Wimmer, H., Richlan, F., Ludersdorfer, P., Klackl, J., Kronbichler, M., 2014. Resting-state and task-based functional brain connectivity in developmental dyslexia. Cereb. Cortex. http://dx.doi.org/10.1093/cercor/bhu184.
Shaywitz, S.E., Shaywitz, B.A., Pugh, K.R., Fulbright, R.K., Constable, R.T., Mencl, W.E., Shankweiler, D.P., Liberman, A.M., Skudlarski, P., Fletcher, J.M., Katz, L., Marchione, K.E., Lacadie, C., Gatenby, C., Gore, J.C., 1998. Functional disruption in the organization of the brain for reading in dyslexia. Proc. Natl. Acad. Sci. U. S. A. 95, 2636–2641.
Sheppard, J.P., Wang, J.P., Wong, P.C., 2012. Large-scale cortical network properties predict future sound-to-word learning success. J. Cogn. Neurosci. 24, 1087–1103.
Sporns, O., 2011. The non-random brain: efficiency, economy, and complex dynamics. Front. Comput. Neurosci. 5, 5.
Spreng, R.N., 2012. The fallacy of a "task-negative" network. Front. Psychol. 3.
Tatsuno, Y., Sakai, K.L., 2005. Language-related activations in the left prefrontal regions are differentially modulated by age, proficiency, and task demands. J. Neurosci. 25, 1637–1644.

Tomasi, D., Volkow, N.D., 2012. Resting functional connectivity of language networks: characterization and reproducibility. Mol. Psychiatry 17, 841–854.
Tomasi, D., Wang, R., Wang, G.J., Volkow, N.D., 2014. Functional connectivity and brain activation: a synergistic approach. Cereb. Cortex 24, 2619–2629.
Tzourio-Mazoyer, N., Landeau, B., Papathanassiou, D., Crivello, F., Etard, O., Delcroix, N., Mazoyer, B., Joliot, M., 2002. Automated anatomical labeling of activations in SPM using a macroscopic anatomical parcellation of the MNI MRI single-subject brain. NeuroImage 15, 273–289.
Uehara, T., Yamasaki, T., Okamoto, T., Koike, T., Kan, S., Miyauchi, S., Kira, J.I., Tobimatsu, S., 2014. Efficiency of a "small-world" brain network depends on consciousness level: a resting-state fMRI study. Cereb. Cortex 24, 1529–1539.
Vigneau, M., Beaucousin, V., Herve, P.Y., Duffau, H., Crivello, F., Houde, O., Mazoyer, B., Tzourio-Mazoyer, N., 2006. Meta-analyzing left hemisphere language areas: phonology, semantics, and sentence processing. NeuroImage 30, 1414–1432.
Vigneau, M., Beaucousin, V., Herve, P.Y., Jobard, G., Petit, L., Crivello, F., Mellet, E., Zago, L., Mazoyer, B., Tzourio-Mazoyer, N., 2011. What is right-hemisphere contribution to phonological, lexico-semantic, and sentence processing? Insights from a meta-analysis. NeuroImage 54, 577–593.
Vincent, J.L., Kahn, I., Snyder, A.Z., Raichle, M.E., Buckner, R.L., 2008. Evidence for a frontoparietal control system revealed by intrinsic functional connectivity. J. Neurophysiol. 100, 3328–3342.
Vogel, A.C., Miezin, F.M., Petersen, S.E., Schlaggar, B.L., 2012a. The putative visual word form area is functionally connected to the dorsal attention network. Cereb. Cortex 22, 537–549.
Vogel, A.C., Petersen, S.E., Schlaggar, B.L., 2012b. The left occipitotemporal cortex does not show preferential activity for words. Cereb. Cortex 22, 2715–2732.
Vogel, A.C., Church, J.A., Power, J.D., Miezin, F.M., Petersen, S.E., Schlaggar, B.L., 2013. Functional network architecture of reading-related regions across development. Brain Lang. 125, 231–243.
Wang, J., Wang, L., Zang, Y., Yang, H., Tang, H., Gong, Q., Chen, Z., Zhu, C., He, Y., 2009. Parcellation-dependent small-world brain functional networks: a resting-state fMRI study. Hum. Brain Mapp. 30, 1511–1523.
Wartenburger, I., Heekeren, H.R., Abutalebi, J., Cappa, S.F., Villringer, A., Perani, D., 2003. Early setting of grammatical processing in the bilingual brain. Neuron 37, 159–170.
Watts, D.J., Strogatz, S.H., 1998. Collective dynamics of 'small-world' networks. Nature 393, 440–442.
Wei, T., Liang, X., He, Y., Zang, Y., Han, Z., Caramazza, A., Bi, Y., 2012. Predicting conceptual processing capacity from spontaneous neuronal activity of the left middle temporal gyrus. J. Neurosci. 32, 481–489.
Wen, X., Liu, Y., Yao, L., Ding, M., 2013. Top-down regulation of default mode activity in spatial visual attention. J. Neurosci. 33, 6444–6453.
Xia, M., Wang, J., He, Y., 2013. BrainNet Viewer: a network visualization tool for human brain connectomics. PLoS One 8, e68910.
Xiang, H.D., Fonteijn, H.M., Norris, D.G., Hagoort, P., 2010. Topographical functional connectivity pattern in the perisylvian language networks. Cereb. Cortex 20, 549–560.
Ye, Z., Zhou, X.L., 2009. Executive control in language processing. Neurosci. Biobehav. Rev. 33, 1168–1177.
Yeo, B.T., Krienen, F.M., Sepulcre, J., Sabuncu, M.R., Lashkari, D., Hollinshead, M., Roffman, J.L., Smoller, J.W., Zollei, L., Polimeni, J.R., Fischl, B., Liu, H., Buckner, R.L., 2011. The organization of the human cerebral cortex estimated by intrinsic functional connectivity. J. Neurophysiol. 106, 1125–1165.
Yokoyama, S., Okamoto, H., Miyamoto, T., Yoshimoto, K., Kim, J., Iwata, K., Jeong, H., Uchida, S., Ikuta, N., Sassa, Y., Nakamura, W., Horie, K., Sato, S., Kawashima, R., 2006. Cortical activation in the processing of passive sentences in L1 and L2: an fMRI study. NeuroImage 30, 570–579.
Zhang, J., Wang, J., Wu, Q., Kuang, W., Huang, X., He, Y., Gong, Q., 2011. Disrupted brain connectivity networks in drug-naive, first-episode major depressive disorder. Biol. Psychiatry 70, 334–342.
Zhu, Z., Feng, G., Zhang, J.X., Li, G., Li, H., Wang, S., 2013. The role of the left prefrontal cortex in sentence-level semantic integration. NeuroImage 76, 325–331.